Investigating the molecular underpinnings underlying morphology and changes in carbon partitioning during tension wood formation in *Eucalyptus*

Eshchar Mizrachi[1], Victoria J. Maloney[2], Janine Silberbauer[1], Charles A. Hefer[3], Dave K. Berger[4], Shawn D. Mansfield[2] and Alexander A. Myburg[1]

[1]Department of Genetics, Forestry and Agricultural Biotechnology Institute (FABI), University of Pretoria, Private bag X20, Pretoria 0028, South Africa; [2]Department of Wood Science, University of British Columbia, 4030-2424 Main Mall, Vancouver, BC V6T 1Z4, Canada; [3]Bioinformatics and Computational Biology Unit, Department of Biochemistry, University of Pretoria, Private Bag X20, Pretoria 0028, South Africa; [4]Department of Plant Science, Forestry and Agricultural Biotechnology Institute (FABI), University of Pretoria, Pretoria 0002, South Africa

Author for correspondence:
Alexander A. Myburg
Tel: +27 12 420 4945
Email: zander.myburg@up.ac.za

Key words: cellulose, *Eucalyptus*, hemicellulose, lignin, RNA-seq, tension wood, transcriptome, xylan.

Summary

- Tension wood has distinct physical and chemical properties, including altered fibre properties, cell wall composition and ultrastructure. It serves as a good system for investigating the genetic regulation of secondary cell wall biosynthesis and wood formation. The reference genome sequence for *Eucalyptus grandis* allows investigation of the global transcriptional reprogramming that accompanies tension wood formation in this global wood fibre crop.
- We report the first comprehensive analysis of physicochemical wood property changes in tension wood of *Eucalyptus* measured in a hybrid (*E. grandis* × *Eucalyptus urophylla*) clone, as well as genome-wide gene expression changes in xylem tissues 3 wk post-induction using RNA sequencing.
- We found that *Eucalyptus* tension wood in field-grown trees is characterized by an increase in cellulose, a reduction in lignin, xylose and mannose, and a marked increase in galactose. Gene expression profiling in tension wood-forming tissue showed corresponding down-regulation of monolignol biosynthetic genes, and differential expression of several carbohydrate active enzymes.
- We conclude that alterations of cell wall traits induced by tension wood formation in *Eucalyptus* are a consequence of a combination of down-regulation of lignin biosynthesis and hemicellulose remodelling, rather than the often proposed up-regulation of the cellulose biosynthetic pathway.

Introduction

Tension wood formation is a dicot-specific physiological reaction to mechanical or gravimetric stress on the tree. The biology of tension wood is still not fully understood, but evidence suggests that transcriptional and metabolic reprogramming contributes significantly to the early induction and establishment of the developmental programme and the later stable formation of wood with altered chemical composition and ultrastructure. As tension wood formation is associated with a trend towards decreased lignin and increased cell wall polysaccharides (Al-Haddad *et al.*, 2013), it presents a relevant model in which to investigate the molecular underpinnings of carbon allocation and carbohydrate deposition in wood. While most genome-wide gene expression and wood physicochemical analyses have thus far been performed in *Populus* species and hybrids (Andersson-Gunneråsa *et al.*, 2006), the availability of a genome from a second forest tree species, *Eucalyptus grandis* (Myburg *et al.*, 2014), facilitates comparative studies to better understand the biology of tension wood formation in a woody plant that has evolved independently from other sequenced plants for > 100 million yr, with a large part of this independent evolution occurring in complete isolation on the Australian continent.

Tension wood possesses distinct physical and chemical properties. Reported physical changes in tension wood include longer vessels (Jourez *et al.*, 2001), longer and thinner fibres (Yoshizawa *et al.*, 2000; Jourez *et al.*, 2001) – possessing a thicker cell wall and smaller lumen – and a higher fibre : vessel ratio compared with normal or opposite wood (Jourez *et al.*, 2001; Ruelle *et al.*, 2006). The vessels and fibres are also typically more compact in tension wood, such that the middle lamellae possess a smaller surface area (Bowling & Vaughn, 2008). Within the secondary cell walls (SCWs) of tension wood fibres, there are marked differences in cellulose properties. Typically, α-cellulose is relatively increased in tension wood (Côté *et al.*, 1969; Okuyama *et al.*, 1994; Yoshizawa *et al.*, 2000), and the cellulose is more

crystalline (Okuyama *et al.*, 1994; Muller *et al.*, 2006) and has a marked decrease in microfibril angle (MFA; Okuyama *et al.*, 1994; Washusen *et al.*, 2005; Ruelle *et al.*, 2006, 2010; Clair *et al.*, 2011).

In some cases, the traditional three-layered (S_1, S_2 and S_3) secondary cell wall layers are often reported to be partially replaced by a gelatinous layer (G-layer) in tension wood, although this is not obligatory, and varies between and within angiosperm species (Washusen *et al.*, 2003; Clair *et al.*, 2006b; Qiu *et al.*, 2008; Ruelle *et al.*, 2010). It is also debatable whether the G-layer is the causal agent of generating the tension (Okuyama *et al.*, 1994; Yamamoto, 2004; Fang *et al.*, 2007, 2008; Goswami *et al.*, 2008) or a physiological byproduct of xylem reprogramming in some species (Washusen *et al.*, 2003; Clair *et al.*, 2006a; Qiu *et al.*, 2008). However, in all cases tension wood is characterized by a relative increase in cell wall glucose in the form of cellulose, a decrease in lignin (Bentum *et al.*, 1969; Okuyama *et al.*, 1994; Aoyama *et al.*, 2001; Yoshida *et al.*, 2002), and an increase in the syringyl:guaiacyl (S:G) lignin monomer ratio (Aoyama *et al.*, 2001; Yoshida *et al.*, 2002; Joseleau *et al.*, 2004). Similarly, the hemicellulose composition changes, and may be variable, especially with the presence/absence of a G-layer. Previous reports have highlighted the putative roles of xyloglucan (Nishikubo *et al.*, 2007; Mellerowicz *et al.*, 2008; Baba *et al.*, 2009), pectinacious compounds (Andersson-Gunneråas *et al.*, 2006; Goulao *et al.*, 2011) such as rhamnogalacturonan I (RG I) (Bowling & Vaughn, 2008) and other galactose-containing polysaccharides such as those found in arabinogalactan proteins (AGPs) (Lafarguette *et al.*, 2004; Andersson-Gunneråas *et al.*, 2006; Bowling & Vaughn, 2008) in generating or facilitating tension wood formation. The orientation of cellulose microfibrils has been suggested to be influenced by galactan, which (either as a component of AGPs or as high-molecular-weight galactan) has been implicated in cellulose orientation during S_2 deposition in other fibres with a G-layer-rich physiology, such as flax phloem fibres (Gorshkova & Morvan, 2006; Roach *et al.*, 2011).

The most detailed study of the physiological and molecular responses to tension wood to date has been performed by Andersson-Gunneråas *et al.* (2006), who examined transcriptional and metabolomic responses of G-layer-forming tension wood in *P. tremula* 3 wk post tension wood induction. Primarily focusing on carbohydrate metabolism, these authors showed that, while the expression of cellulose synthase genes was not necessarily affected at the transcriptional level, the differential regulation of genes belonging to several key pathways was indicative of the change in carbon allocation favouring biosynthesis of cellulose over other cell wall moieties. For example, significant decreases in GDP sugar channelling to mannan biosynthesis and the pentose phosphate pathway were observed (Andersson-Gunneråas *et al.*, 2006).

Several studies have also consistently found evidence of key hormone signalling pathways affected in tension wood-forming tissue, such as the activation of ethylene-mediated pathways (Andersson-Gunneråas *et al.*, 2003, 2006; Vahala *et al.*, 2013). Ethylene is known to be an inducer of cambial growth (Love *et al.*, 2009), and has been shown in *Zinnia elegans* to be mass-produced in late-maturing tracheary elements (TEs) and diffuse in a paracrine fashion (i.e. influencing any immediately surrounding cells) to modulate additional TE differentiation from the cambium, coordinating both axial and radial vascular development (Pesquet & Tuominen, 2011). Auxin maintains cambial initials in an undifferentiated form, while polar auxin transport and localized auxin suppression are associated with cambial differentiation (Moyle *et al.*, 2002; Ko *et al.*, 2004; Baba *et al.*, 2011). Gibberellins have also been shown to act synergistically with auxin to promote cambial differentiation and fibre elongation (Little & Savidge, 1987), and the production of gibberellic acid (GA) and auxins induces similar responses at the transcriptional level (Björklund *et al.*, 2007). The synergistic mechanism is probably governed by the influence of GA on the polar transport of auxin (reviewed in Elo *et al.*, 2009). Several hormones, and particularly GA, have also been linked to cortical microtubule arrangement during cellulose deposition, indirectly influencing cellulose properties (Lloyd, 2011). For example, jasmonic acid (JA) signalling has been linked to cells under tension, showing up-regulation of the mechano-inducible *JASMONATE ZIM-domain 10* (*JAZ10*) gene in the interfascicular fibres of *Arabidopsis thaliana* (Sehr *et al.*, 2010). JA signalling was shown to stimulate secondary growth of cambial initials (Sehr *et al.*, 2010), although this aspect has not yet been adequately studied in a woody species.

Despite extensive research on tension wood formation, much has not been resolved concerning the physicochemical changes in tension wood in *Eucalyptus*, and it is not known whether the changes in tension wood would result in a similar phenotype to that observed in other woody angiosperms, such as *Populus*. Previously, Paux *et al.* (2005) and Qiu *et al.* (2008) reported on variation in the gene expression profiles of 231 genes on a 4900-probe microarray during tension wood formation in *Eucalyptus*. More recently, a focused study of 38 hemicellulose- and pectin-modifying candidate genes was also performed in *Eucalyptus globulus* (Goulao *et al.*, 2011). Considering the extent of gene duplication and the roles of potential paralogues, it is crucial to obtain a transcriptome-wide view of the transcriptional response, as expression profiling of individual paralogues may be misleading. As xylogenesis is known to be regulated to a large extent at a transcriptional level, it would be interesting to see if tension wood formation results in similar transcriptional reprogramming that explains the changes in phenotype, and may highlight important genes or regulatory elements that have not previously been identified. This could be beneficial to industrial applications such as pulp, paper, timber and biofuel production, as they would offer targets for selection in breeding programmes or candidates for genetic manipulation.

In this study, we aimed to investigate the physical effects observed in mature tension wood-forming tissue of a widely grown hybrid *Eucalyptus* genotype (*Eucalyptus grandis* × *Eucalyptus urophylla*). We further aimed to provide a detailed, whole-transcriptome characterization of *Eucalyptus* tension wood-forming tissue at 3 wk post induction by mRNA sequencing to investigate the transcriptional reprogramming that occurs during stable tension wood formation. We hypothesized that

the transcriptional response in *Eucalyptus* should reflect the rapid differentiation of longer, thinner fibre cells, which should be accompanied by evidence of a flux of auxin-mediated pathways and the up-regulation of ethylene- and GA-mediated pathways, as well as an increase in pectic degradation, rapid cell elongation and altered programmed cell death, to reflect this fibre phenotype.

Materials and Methods

Sampling for wood property analysis

To characterize the physicochemical properties of tension wood in *Eucalyptus* trees and to obtain enough tissue for wood chemistry analysis, we collected basal sections of naturally leaning branches from five different ramets of the same 3–4 yr-old F_1 *Eucalyptus grandis* (Hill ex Maiden) × *Eucalyptus urophylla* (S.T. Blake) hybrid clone (GUSAP1; Sappi Forest Research, KwaMbonambi, South Africa; Supporting Information Fig. S1). A section of the leaning stems of each of the five trees was analysed where the angle was 45° in relation to the main trunk of the tree. For each tree, sections were compared between the side closer to the main trunk (top of the branch; tension wood-forming) and the side opposite to that (opposite wood-forming). This provided a sample of woody material produced by stable tension wood formation (i.e. not recently induced).

Klason lignin determination

Wood was ground in a Wiley mill (Thomas Scientific, Philadelphia, PA, USA) to pass a 0.4-mm screen (40 mesh) and Soxhlet extracted overnight in hot acetone to remove extractives. Lignin and carbohydrate contents were determined with a modified Klason (Coleman *et al.*, 2009) method in which extracted ground stem tissue (100 mg) was treated with 3 ml of 72% H_2SO_4 and stirred every 10 min for 2 h. Samples were then diluted with 112 ml of deionized water and autoclaved for 1 h at 121°C. The acid-insoluble lignin fraction was determined gravimetrically by filtration through a pre-weighed medium-coarseness sintered-glass crucible, while the acid-soluble lignin component was determined spectrophotometrically by absorbance at 205 nm. Carbohydrate contents were determined using an anion exchange high-performance liquid chromatograph (Dx-600; Dionex, Sunnyvale, CA, USA) equipped with an ion exchange PA1 (Dionex) column, a pulsed amperometric detector with a gold electrode, and a SpectraAS3500 auto injector (Spectra-Physics, Santa Clara, CA, USA).

α-cellulose content determination

The holocellulose content was determined using a modified version of the method of Browning (1967). Briefly, 200 mg of extracted ground wood was de-lignified by adding 3.5 ml of buffer solution (60 ml of glacial acetic acid + 1.3 g $NaOH\,l^{-1}$) and 1.5 ml of 20% sodium chlorite solution (20 g $NaClO_2$ in 80 ml of distilled water) then gently shaken at 50°C overnight (14–16 h). The following day the reaction was quenched by placing it into an ice bath and incubating it at 4°C for several hours before the reaction solution was removed and a second reaction was performed overnight. Finally, the reacted wood meal was transferred to a pre-weighed coarse sintered-glass crucible and washed twice with 50 ml of 1% glacial acetic acid followed by a single wash with 10 ml of acetone under suction. The resulting holocellulose was permitted to dry in a 50°C oven overnight and the percentage of total extracted ground wood was determined gravimetrically. The α-cellulose content was then determined by extracting 80 mg of the oven-dried holocellulose with 4 ml of 17.5% sodium hydroxide for 30 min at room temperature then adding 4 ml of water, stirring for 1 min and leaving it to react for another 29 min. The reaction solution was then filtered through a pre-weighed coarse sintered-glass crucible, washed with deionized water (3 × 50 ml), soaked in 1.0 M acetic acid for 5 min and washed again with deionized water (3 × 50 ml). Finally, the samples were dried at 50°C overnight and the percentage of total holocellulose was determined gravimetrically (Yokoyama *et al.*, 2002).

Microfibril angle determination

Microfibril angle estimates were generated by X-ray diffraction (Ukrainetz *et al.*, 2008). The 002 diffraction spectra were screened for T-value distribution and symmetry on a Bruker D8 discover X-ray diffraction unit (Bruker-ASX, Madison WI, USA) equipped with an general area array detector (GADDS; Bruker). Wide-angle diffraction was used in the transmission mode, and the measurements were performed with CuKα1 radiation (λ = 1.54 Å). The X-ray source was fitted with a 0.5-mm collimator, and the scattered photons were collected by a GADDS detector. Both the X-ray source and detector were set to theta = 0°.

Calcofluor staining for cellulose

Samples were radially cut into 20-μm cross-sections using a Leica SM2000r hand sliding microtome (Leica Microsystems, Wetzlar, Germany) and stored in dH_2O until needed. Sections were treated with 0.01% calcofluor white for 3 min, then washed three times to remove excess stain (Falconer & Seagull, 1985). All sections were mounted onto glass slides and examined with a Leica DRM microscope (Leica Microsystems) fitted with epifluorescence optics. Photographs were taken with a QICAM camera (QImaging, Surrey, Canada) and OpenLab software (PerkinElmer Inc., Waltham, MA, USA). Images were visualized and analysed using ImageJ software (Abràmoff *et al.*, 2004).

Tension wood induction and sampling of differentiating xylem for transcriptome analysis

A tree bending trial was conducted in a clonal field trial near KwaMbonambi in Northern Kwazulu-Natal, South Africa (Sappi Forest Research) to induce tension wood formation in ramets of the same F1 clone (GUSAP1) as used for wood property analyses.

The main stems of three 18-month-old ramets of the clone were bent at an angle of *c.* 45° for 3 wk in the field. To avoid temporal variation in gene expression, sampling of all replicates was completed within 3 h around noon on the same day under the same environmental conditions. Differentiating xylem tissue was isolated from the section of the stem bent at 45° (*c.* 50 cm), removing the bark and immediately scraping the exposed outer differentiating layers of xylem cells 4–5 mm deep. For each bent stem, the upper (tension wood) side was scraped. Differentiating xylem was collected from the corresponding location (height from the base) on three unbent controls. All samples were immediately frozen in liquid nitrogen and stored at −80°C.

RNA isolation, sequencing and analysis

Total RNA was isolated from the xylem samples using a cetyl trimethylammonium bromide (CTAB)-based method (Chang *et al.*, 1993). Frozen wood samples were ground to a fine powder in liquid nitrogen using a high-speed grinder (IKA-Werke, Staufen, Germany). Fifteen millilitres of extraction buffer was mixed with 3 g of ground tissue. RNA quantity and purity were assessed using a Nanodrop spectrophotometer (Nanodrop Technologies ND 1000, Wilmington, DE, USA), Agilent Bioanalyser 2100 RNA 6000 pico total RNA kits (Agilent Technologies, Santa Clara, CA, USA) and 1.5% RNase-free agarose gels. To qualify for mRNA-Seq library preparation, all RNA samples had to have RNA integrity (RIN) numbers (Schroeder *et al.*, 2006) of 8.0 or higher. In addition, the samples were tested for DNA contamination using an intron-spanning PCR. RNA from three biological replicates each of tension wood and upright control samples was sequenced (paired-end, 80 bp–80 bp) and mapped to the *E. grandis* genome using TOPHAT (Trapnell *et al.*, 2009) version 1.3.1, with the JGI V.02 gene models as a reference (www.phytozome.net). Total mapped reads varied from *c.* 8 million to 20 million between samples (Supporting Information Table S1). Expression levels (fragments per kilobase of coding sequence per million mapped fragments (FPKM)) were calculated differentially expressed genes were identified using the CUFFLINKS and CUFFDIFF packages, version 1.0.3 (Trapnell *et al.*, 2010). Aligned reads have been submitted to the Sequence Read Archive (SRA) (Leinonen *et al.*, 2010) under project code SRP047282.

Results

Physicochemical changes of tension wood in *Eucalyptus*

We assessed changes in wood properties in naturally occurring tension wood derived from plantation-grown trees. To do this we collected tension and opposite wood from leaning basal side branches of five different ramets of an *E. grandis* × *E. urophylla* clone (GUSAP1; Sappi Forest Research; Fig. S1). Physical, chemical and ultrastructural characteristics of the tension wood and opposite wood were measured and compared (Table 1). In accordance with the individually quantified fibre characteristics, a marked difference in cell wall thickness between tension wood and opposite wood was observable by microscopy (Figs 1, S2). In the tension wood, fibres were on average 20% longer and showed a 40% increase in fibre coarseness. Fibre width was not significantly changed, but the secondary cell walls were thicker, consistent with the coarseness estimates. The fibre:vessel ratio was also higher in the tension wood (vessel density was 33% lower in tension wood), while vessel length and width were not significantly different.

In addition to the physical wood measurements, chemical analysis of the wood was performed to quantify changes in cellulose properties (Table 2), as well as lignin and total cell wall carbohydrate differences compared with opposite wood (Table 3). Although wood density and holocellulose (total polysaccharide) content were not different between tension and opposite wood, there was a significant increase in relative glucose content (*c.* 6 mg 100 mg^{-1} or a 16% relative increase) in the tension wood. This was mainly attributable to a relative increase in cellulose, as reflected in the significant increase in the α-cellulose content of the tension wood (Table 2). Consistent with previous tension wood studies, we also found a lower MFA in the tension wood (20% decrease). The hemicellulose composition was also

Table 1 Fibre and vessel properties in tension and opposite wood of five ramets of *Eucalyptus grandis* × *Eucalyptus urophylla* F_1 hybrid clone GUSAP1

Sample	Fibre length (mm)	Fibre width (μm)	Fibre coarseness (mg m^{-1})	Vessel area (mm^2)	Vessel length (mm)	Vessel width (μm)	Vessels m^{-1} (*n*)
Opposite wood 1	0.78	18.50	0.03	0.07	0.57	118.30	8.58
Opposite wood 2	0.69	19.20	0.04	0.06	0.54	107.20	10.12
Opposite wood 3	0.62	19.10	0.05	0.06	0.51	112.70	9.88
Opposite wood 4	0.77	19.20	0.06	0.06	0.54	114.20	7.99
Opposite wood 5	0.70	18.20	0.06	0.05	0.49	105.40	9.69
Tension wood 1	0.88	17.90	0.06	0.07	0.56	118.30	7.55
Tension wood 2	0.75	19.20	0.05	0.07	0.57	121.30	6.61
Tension wood 3	0.85	17.40	0.06	0.06	0.57	109.10	4.66
Tension wood 4	0.88	18.40	0.06	0.07	0.56	124.50	6.77
Tension wood 5	0.87	18.60	0.06	0.07	0.55	121.40	4.75
Opposite wood (mean ± SD)	0.70 ± 0.06	18.84 ± 0.46	0.05 ± 0.01	0.06 ± 0.01	0.53 ± 0.03	111.56 ± 5.26	9.25 ± 0.92
Tension wood (mean ± SD)	0.85 ± 0.05**	18.30 ± 0.69	0.06 ± 0.00*	0.07 ± 0.00	0.56 ± 0.01	118.92 ± 0.07	6.07 ± 1.29**

Vessels m^{-1} indicates the density of vessels, calculated as the number (*n*) of observed vessels. Paired, two-tailed *t*-test: *, $P \leq 0.05$; **, $P \leq 0.01$.

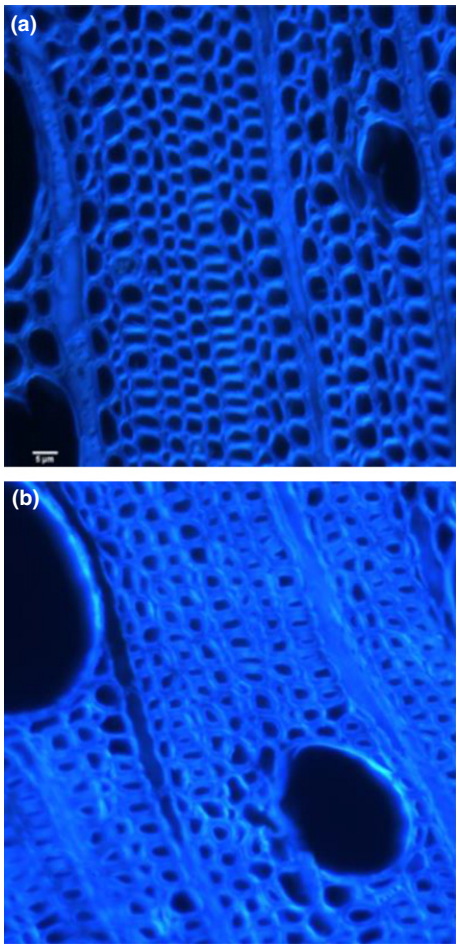

Fig. 1 Cell wall morphology of opposite wood (a) and tension wood (b) from an *Eucalyptus grandis* × *Eucalyptus urophylla* hybrid tree (ramet). Comparisons for all sampled ramets (Supporting Information Fig. S1) can be seen Fig. S2. Bar, 5 μm.

different between tension and opposite wood. In short, rhamnose and arabinose were not significantly different and showed the highest variation among trees, but xylose and mannose concentrations were significantly lower in tension wood. However, the largest difference in tension wood hemicellulose was in galactose content, which was *c.* 300% higher in tension wood (mean 1.82 mg 100 mg^{-1} DW compared with 0.58 mg 100 mg^{-1} in opposite wood). The insoluble lignin content was also significantly reduced in tension wood compared with opposite wood (by 4.34%, to 26.2 g 100 g^{-1} DW). A summary of the differences in all wood properties can be seen in Fig. 2 and Tables S2 and S3.

Transcriptional response to induced tension wood formation

To profile differential gene expression in tension wood-forming tissues, we collected xylem from three 18-month-old GUSAP1 trees that were bent for 3 wk. This experimental design permitted comparison with previous tension wood profiling experiments in *Populus* (Andersson-Gunnerås *et al.*, 2006; Jin *et al.*, 2011). However, the actual bending and sampling were performed in field-grown *Eucalyptus* trees, in this case, as opposed to potted glasshouse-grown poplar trees. Additional trees of the same age that had been bent in the same manner for 6 months in the field demonstrated observable tension wood at a macroscopic level (Fig. S3). RNA was extracted and RNA-seq (Illumina, San Diego, CA, USA) data produced from the xylem of three biological replicates of tension wood-forming trees (3 wk post-induction) and upright controls. Overall, we found 366 genes that were significantly ($q < 0.05$) differentially expressed in tension wood compared with the upright control sample (176 up-regulated and 190 down-regulated; Fig. S4, Tables S4, S5). *Arabidopsis thaliana* gene IDs homologous to the *Eucalyptus* gene IDs according to the *E. grandis* V.02 annotation (www.phytozome.net) were used for analysis using the BiNGO (Maere *et al.*, 2005) and GOToolBox (Martin *et al.*, 2004) tools to identify overrepresentation of ontology terms in the differentially expressed genes (Figs S5, S6, Table S6).

In general, the most enriched biological processes in tension wood were genes related to the stress response (stress, chemical, abiotic and mechanical stimuli). In addition, and consistent with previous analyses of differentially regulated genes in tension

Table 2 Basic wood density, holocellulose, α-cellulose and microfibril angle in tension and opposite wood of five ramets of *Eucalyptus grandis* × *Eucalyptus urophylla* F_1 hybrid clone GUSAP1

Sample	Wood density (kg m^{-3})	Holocellulose (mg 100 mg^{-1})	α-Cellulose (mg 100 mg^{-1})	Microfibril angle (°)
Opposite wood 1	460.28	64.35	38.29	21.23
Opposite wood 2	411.74	63.92	38.96	19.31
Opposite wood 3	504.38	65.28	37.29	18.42
Opposite wood 4	465.49	67.10	39.62	22.12
Opposite wood 5	531.19	65.24	40.47	18.55
Tension wood 1	483.04	64.34	41.86	15.23
Tension wood 2	413.49	62.81	39.66	16.25
Tension wood 3	516.17	66.68	41.93	14.33
Tension wood 4	507.82	71.61	42.04	14.59
Tension wood 5	483.78	69.97	40.14	15.48
Opposite wood (mean ± SD)	474.62 ± 45.63	65.18 ± 1.22	38.93 ± 1.22	19.92 ± 0.74
Tension wood (mean ± SD)	480.86 ± 40.39	67.08 ± 3.70	41.13 ± 1.13*	15.18 ± 0.34**

Paired, two-tailed *t*-test: *, $P \leq 0.05$; **, $P \leq 0.01$.

Table 3 Cell wall composition in tension and opposite wood of five ramets of *Eucalyptus grandis* × *Eucalyptus urophylla* F_1 hybrid clone GUSAP1

	Content (mg 100 mg^{-1})								
	Acid-insoluble lignin	Acid-soluble lignin	Total lignin	Arabinose	Rhamnose	Galactose	Glucose	Xylose	Mannose
Opposite wood 1	26.66	2.74	29.40	0.44	0.30	0.51	42.45	13.39	2.25
Opposite wood 2	28.52	2.48	31.01	0.45	0.35	0.69	42.41	13.45	2.47
Opposite wood 3	26.97	2.76	29.74	0.37	0.33	0.59	41.86	13.45	2.90
Opposite wood 4	27.09	2.51	29.60	0.31	0.20	0.43	44.15	14.63	2.63
Opposite wood 5	27.94	2.55	30.49	0.20	0.31	0.67	39.29	11.23	2.39
Tension wood 1	26.67	2.86	29.53	0.41	0.08	1.38	48.27	11.19	1.47
Tension wood 2	26.61	2.68	29.29	0.32	0.25	1.75	49.26	11.16	1.82
Tension wood 3	25.67	2.76	28.42	0.35	0.27	1.77	48.07	10.47	1.54
Tension wood 4	26.18	2.59	28.77	0.36	0.36	1.72	48.20	10.73	1.56
Tension wood 5	26.03	2.40	28.44	0.34	0.35	2.47	50.17	10.07	1.65
Opposite wood (mean ± SD)	27.44 ± 0.77	2.61 ± 0.13	30.05 ± 0.68	0.36 ± 0.10	0.30 ± 0.06	0.58 ± 0.11	42.03 ± 1.76	13.23 ± 1.23	2.53 ± 0.25
Tension wood (mean ± SD)	26.23 ± 0.42*	2.66 ± 0.18	28.89 ± 0.50*	0.36 ± 0.03	0.26 ± 0.11	1.82 ± 0.40**	48.79 ± 0.90**	10.73 ± 0.47**	1.61 ± 0.13**

Paired, two-tailed *t*-test: *, $P \leq 0.05$; **, $P \leq 0.01$.

Fig. 2 Relative changes in wood properties between tension wood and opposite wood in five ramets of *Eucalyptus grandis* × *Eucalyptus urophylla* F_1 hybrid clone GUSAP1. A positive change indicates a higher value in tension wood as compared with opposite wood, and a negative change indicates a lower value in tension wood compared with opposite wood. Error bars represent ± SE ($n = 5$). Paired, two-tailed *t*-test: *, $P \leq 0.05$.

wood, several genes coding for FASCICLIN-LIKE ARABINOGALACTAN (FLA) proteins were highly up-regulated – *FLA11* (*Eucgr.B02486*), *FLA12* (*Eucgr.J00938*) and *FLA17* (*Eucgr.A02551*) homologues. Other cell wall signalling-related genes were up-regulated, including two homologues of leucine-rich repeat protein kinases (*Eucgr.F02727* and *Eucgr.L02854*), annexin (*Eucgr.F02423*), IQ-Domain10 (*IQD10*; *Eucgr.F01203*) and a RAB GTPase homologue (*Eucgr.B02741*). Homologues of several transcription factors that have previously been associated with SCW biosynthesis were also up-regulated, including *KNOTTED-LIKE HOMEOBOX OF ARABIDOPSIS THALIANA 7* (*KNAT7*) (*Eucgr.D01935*), *MYB52* (*Eucgr.F02756*), a C3HC4-type RING finger zinc finger family protein (*Eucgr.I01697*) and two C2H2-like zinc finger proteins (*Eucgr.B02487* and *Eucgr.H00574*). The joint up-regulation of *KNAT7* and *MYB52* is interesting, as these genes have been shown to be co-regulated in *A. thaliana* and are both repressed by MYB7 (Ko *et al.*, 2009), an orthologue of which (*Eucgr.C00721*) was down-regulated in the tension wood (Table S4). A homologue of *MYB61* (*Eucgr.B02197*) was also up-regulated. In *A. thaliana* this gene has been shown to be expressed in sink tissues, and is essential for xylem formation (Romano *et al.*, 2012). Other than general stress response-related ontologies, the only other categories enriched in the significantly up-regulated genes were 'positive regulation of cell death' (GO:0010942 and its child terms); 'disaccharide metabolism' (GO:0005984 and its child terms), relating to sucrose and trehalose metabolism; and 'methionine biosynthesis' (GO:0006555; Fig. S5, Table S6).

By contrast, enriched ontologies for down-regulated genes included phenylpropanoid and flavonoid biosynthesis, as well as the biosynthesis of phenylalanine, tyrosine and tryptophan (Fig. S6). Homologues of genes representing most of the

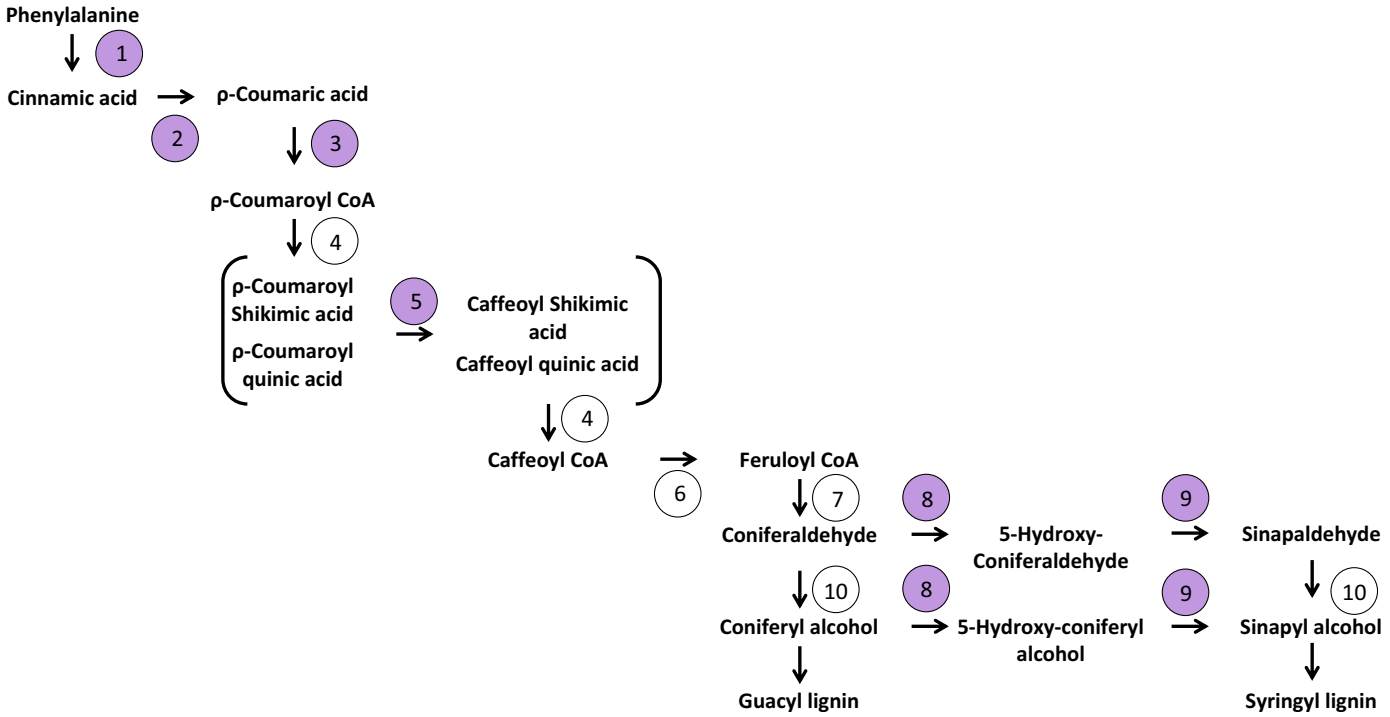

Fig. 3 Main steps of the monolignol biosynthetic pathway in *Eucalyptus* down-regulated in tension wood. Pathway construction is based on Humphreys & Chapple (2002). Enzymatic steps where one or more representative genes showed significant down-regulation in tension wood xylem compared with the upright control in the *Eucalyptus grandis* × *Eucalyptus urophylla* hybrid clone are highlighted in purple. A full table of differential expression for all genes involved in the pathway (annotation according to V. Carocha *et al.*, in preparation) is available in Supporting Information Table S7. Steps 1–10 represent the following reactions: 1, phenylalanine ammonia-lyase (PAL); 2, cinnamate 4-hydroxylase (C4H); 3, 4-coumarate:CoA ligase (4CL); 4, p-hydroxycinnamoyl-CoA:quinate shikimate p–hydroxycinnamoyltransferase (HCT); 5, 4-coumarate 3-hydroxylase (C3′H); 6, caffeoyl-CoA O-methyltransferase (CCoAOMT); 7, cinnamoyl-CoA reductase (CCR); 8, ferulate 5-hydroxylase (F5H); 9, caffeic acid/5-hydroxyconiferaldehyde O-methyltransferase (COMT); 10, cinnamyl alcohol dehydrogenase (CAD).

enzymatic steps involved in the monolignol biosynthetic pathway were significantly down-regulated (Fig. 3), including *PAL* (*Eucgr.J00907*), *C4H* (*Eucgr.J01844*), *4CL* (*Eucgr.K00087*), *C3′H* (*Eucgr.G03199*), *F5H* (*Eucgr.J02393*) and *COMT* (*Eucgr.A01397*). Although evidence of large expansions has been noted for some of these gene families in *E. grandis*, 24 core '*bona fide* lignifying' genes have been identified (V. Carocha *et al.*, in preparation). With the exception of the *CAD* genes, most family members of all *bona fide* monolignol biosynthesis genes were down-regulated, although statistical significance was lacking for some (Table S7).

Given that significant increases in glucose, putatively stemming from increased α-cellulose synthesis, were observed, as well as changes in the relative proportion of hemicellulosic components, we specifically examined the differential expression of genes involved in carbohydrate metabolism (Table 4). Among the up-regulated genes, a *SUCROSE SYNTHASE 4* homologue (*SUS4*; *Eucgr.C03199*), *TRAHALOSE-PHOSPHATASE/SYNTHASE 9* (*Eucgr.B02686*) and a gene coding for a trehalose-phosphatase family protein (*Eucgr.B02686*) were significantly up-regulated, which could provide the increased source of UDP-glucose needed to supply the cellulose synthase machinery. Additionally, a β-glucosidase GH1 coding gene (*Eucgr.B00859*) was up-regulated, which could be involved in cellulose modification in the cell wall. Although we saw no significant differences in expression of any of the cellulose synthase (*CesA*) genes, we observed the expression of a tandem duplicate of *EgCesA3* (*Eucgr.C00246*, orthologue of AtCesA7; Ranik & Myburg, 2006) that has not been previously observed in *Eucalyptus* or annotated in the *E. grandis* genome. The tandem duplicate gene codes for an in-frame copy of *Eucgr.C00246*, and is expressed at a similar level (Fig. S7).

Several other genes encoding glycosyl transferases were also up-regulated, including GT32 (α-1,4-glycosyltransferase family protein; *Eucgr.A00510*) and GT35 (glycogen or starch phosphorylase; *Eucgr.J01374*). Another CAZyme gene transcriptionally up-regulated was *GDP-D-mannose 3′,5′-epimerase* (*GME*), known to be involved in ascorbate biosynthesis, pectic polysaccharide biosynthesis, and the general stress response (Wolucka & Van Montagu, 2003; Caffall & Mohnen, 2009; Smirnoff, 2011). Among the three identified possible enzymatic functions, the most commonly ascribed role (EC 5.1.3.18) is the catalytic conversion of GDP-D-mannose to GDP-L-galactose (Major *et al.*, 2005). This is interesting, as tension wood displayed reduced mannose and increased galactose compared with opposite wood (Fig. 2). In general, with the exception of homologues of *SUS4* and *GLUCURONIC ACID SUBSTITUTION OF XYLAN 2* (*GUX2*; *Eucgr.F00232*), most of the CAZyme genes significantly

Table 4 Carbohydrate active enzyme (CAZyme) genes significantly ($q < 0.05$) differentially expressed in 3-wk tension wood (TW) forming xylem of *Eucalyptus grandis* × *Eucalyptus urophylla* trees

E. grandis ID	*Arabidopsis thaliana* homologue	*Arabidopsis thaliana* protein	CAZyme annotation*	Log_e (fold change)	Average FPKM (upright)†	Average FPKM (TW)†
Eucgr.A00510	AT2G38150	α-1,4-glycosyltransferase	GT32	4.24	0	43
Eucgr.H00343	AT1G68470	Exostosin family protein	GT47	3.87	2	143
Eucgr.I01697	AT3G27330	β-1,4-galactosyltransferase	GT92	3.71	3	153
Eucgr.B00354	AT1G23870	ATTPS9, TPS9	GT20	3.00	1	13
Eucgr.I01147	AT1G49710	FUCTB, FUT12	GT10	2.25	14	111
Eucgr.K00865	AT4G15240	Unknown (DUF604)	GT31	1.78	9	71
Eucgr.B00859	AT3G18080	BGLU44	GH1	1.51	10	26
Eucgr.B02686	AT1G68020.2	ATTPS6, TPS6	GT20	1.49	9	36
Eucgr.F03658	AT1G55740	AtSIP1, SIP1	GH36	1.48	10	41
Eucgr.E01169	AT4G19420	PAE8	CE13	1.36	40	121
Eucgr.F01855	AT1G45130	BGAL5	GH35	1.19	5	14
Eucgr.J01374	AT3G29320	α-Glucan phosphorylase	GT35	1.12	5	14
Eucgr.B02118	AT5G28840	GME		1.12	13	38
Eucgr.F00232	AT4G33330	GUX2, PGSIP3	GT8	0.94	101	386
Eucgr.H00536	AT3G17880	HIP, TDX	GT41	0.90	20	43
Eucgr.C03199	AT3G43190	SUS4	GT4	0.49	1144	1614
Eucgr.J02867	AT3G13750	BGAL1	GH35	−0.84	28	10
Eucgr.G02748	AT5G04310	Pectin lyase-like	PL1	−1.00	29	12
Eucgr.G02887	AT5G04310	Pectin lyase-like	PL1	−1.12	11	1
Eucgr.F02205	AT1G58370	ATXYN1, RXF12	CBM22	−1.26	16	5
Eucgr.K03600	AT4G13710	Pectin lyase-like	PL1	−1.26	22	8
Eucgr.A00780	AT5G01930	MAN6	GH5	−1.37	72	20
Eucgr.A00485	AT1G19300	GATL1, PARVUS	GT8	−1.51	196	46
Eucgr.C03207	AT3G43190	ATSUS4, SUS4	GT4	−2.74	10	1

*Annotation of CAZymes according to Yin *et al.* (2012). †Average fragments per kilobase of coding sequence per million mapped fragments (FPKM) of three biological replicates.

up-regulated in tension wood showed very low or no expression in the upright control (Table 4), and there is no indication of transcriptional rewiring of CAZymes' roles normally associated with SCW polysaccharide metabolism, as previously demonstrated in *Populus* (Andersson-Gunneras *et al.*, 2006). The down-regulation of *PARVUS* (*Eucgr.A00485*) is notable, as it could be responsible for the reduction in xylose content observed in tension wood.

Several genes associated with changes in hormone metabolism were also differentially expressed during tension wood formation (Table 5). In short, genes associated with elevated activity in the synthesis of ethylene, GA and jasmonic acid in tension wood relative to the upright control was apparent. One of the most highly up-regulated genes in tension wood (50-fold up-regulation) was a homologue of *ACC OXIDASE 4*|*ETHYLENE FORMING ENZYME* (*ACO4*|*EFE*; *Eucgr.D01368*), which is involved in the final step in ethylene formation from methionine by converting 1-aminocyclopropane-1-carboxylate to ethylene. Interestingly, this was contrasted by an almost complete suppression of an *ACO1* homologue expressed in the upright control

Table 5 Hormone-related genes significantly differentially ($q < 0.05$) expressed in 3-wk tension wood forming xylem of *Eucalyptus grandis* × *Eucalyptus urophylla* trees

E. grandis ID	*Arabidopsis thaliana* homologue	*Arabidopsis thaliana* protein	Log_e (fold change)	Average FPKM* (upright)	Average FPKM* (TW)	Hormonal pathway
Eucgr.B03366	AT5G14920	–	4.05	2	124	Gibberellic acid
Eucgr.D01368	AT1G05010	EFE, ACO4	3.68	15	807	Ethylene
Eucgr.E03916	AT5G47530	–	2.83	5	110	Auxin
Eucgr.H04545	AT1G56220	–	1.62	30	220	Auxin
Eucgr.H03965	AT3G16770	RAP2.3, ATEBP, ERF72, EBP	1.33	12	69	Ethylene
Eucgr.C03183	AT4G33150	LKR,\SDH	1.21	7	17	Jasmonic acid
Eucgr.H03171	AT1G04240	SHY2, IAA3	−1.11	20	7	Auxin
Eucgr.H02914	AT2G33310	IAA13	−1.34	25	10	Auxin
Eucgr.G01769	AT2G21050	LAX2	−1.50	121	39	Auxin
Eucgr.C03886	AT2G19590	ACO1	−3.09	87	4	Ethylene
Eucgr.C02930	AT4G32810	CCD8,MAX4	−6.05	23	0	Auxin

*Average per kilobase of coding sequence per million mapped fragments (FPKM) in three biological replicates.

(*Eucgr.C03886*; Table 5), suggesting that a different family member is recruited for ethylene synthesis in *Eucalyptus* tension wood compared with normal wood. The enzymatic function of ACC OXIDASE has previously been highlighted in tension wood-forming tissues of *Populus*, in producing ethylene to stimulate asymmetrical cambial growth (Andersson-Gunnerås *et al.*, 2003; Love *et al.*, 2009). Of note was the up-regulation of an ethylene response transcription factor, *Eucgr.F03499*, a homologue of *A. thaliana ETHELENE RESPONSE FACTOR 72* (*ERF72*). In *Populus* hybrids, the overexpression of ERF72 orthologues (named PtiERF34 and PtiERF35) caused significant increases in the diameter (either gene) and height (PtiERF35 only) of transgenic trees (Vahala *et al.*, 2013). Similarly, in GA signalling, a homologue of an *A. thaliana* gibberellin-response protein, *Eucgr.B03366*, was highly up-regulated. The largest group of genes related to hormonal response was auxin-response genes, which showed both significant up- and down-regulation. Among these was the down-regulation of an oxireductase (*CAROTENOID CLEAVAGE DIOXYGENASE 8* (*CCD8*); *Eucgr.C02930*) associated with polar auxin transport and the suppression of branching (Auldridge *et al.*, 2006). Given that auxin, GA and ethylene are expected to be globally increased in xylogenic tissue of tension wood, these results are consistent with previous reports of hormonal changes in tension wood formation in *Populus*, suggesting a conserved mechanism between species.

Discussion

Tension wood represents an important developmental state consisting of both altered transcriptional and hormonal regulation, and the coordination of cellular processes recruited to alter cell wall chemical constituents. Although several studies have looked at aspects of tension wood in *Eucalyptus*, most of the information – especially regarding gene expression and biological changes – has been based on studies in *Populus*. It was thus not known if the physiological processes in *Eucalyptus* would be similar to those observed in *Populus*, as no study has as yet looked at the detailed physiology of tension wood formation, or indeed profiled gene expression at whole-transcriptome level during tension wood formation in this genus. In this study, we report the first data investigating transcriptome-wide changes manifested during tension wood formation in field-grown *Eucalyptus* trees, and comprehensively describe the physicochemical changes that accompany this developmental response to mechanical stress in woody stems.

Despite the high variation in transcript abundance, which is expected in experiments on field-grown plants, trends in gene expression supported many of the observed physicochemical changes. The number of significantly differentially expressed genes (366) is similar to the 444 previously reported in a controlled, glasshouse-grown *Populus* study at a similar time-point post induction (Andersson-Gunnerås *et al.*, 2006). It is noteworthy that, among the most significantly differentially expressed genes, several common observations could be made between *Eucalyptus* and *Populus* (Table S8) in terms of up-regulation of ethylene biosynthesis (*EFE/ACO4*) and response (*ERF72*), UDP-glucose production (*SUSY*), transcriptional regulators (*KNAT7*, *MYB52* and *At3g27330* homologs) and cell wall signalling genes (*FLA12*), the reduction in the expression of *PARVUS* which is associated with xylan synthesis, and the down-regulation of most lignin-related genes. This suggests common mechanisms employed by these two woody dicots in regulating and forming tension wood.

In general, the data for morphological and chemical changes concur with those previously obtained in tension wood of various angiosperm species, namely longer fibres, a higher fibre:vessel ratio, relatively increased cellulose with a decreased (smaller relative to the long axis of the fibre) MFA, and a relative decrease in lignin (Tables 1–3). In terms of hemicellulose biosynthesis, we found that, in *Eucalyptus* tension wood, xylan is significantly reduced, and this may be a consequence of the 4-fold down-regulation of the *PARVUS* gene (Table 4). The simultaneous strong up-regulation of a homologue of *GUX2* (*Eucgr.F00232*) in tension wood should also be noted, as *GUX* genes are responsible for glucuronic acid (GlcA) side-chain addition onto the xylan backbone (Mortimer *et al.*, 2010; Lee *et al.*, 2012). It would be interesting to further characterize tension wood xylan to see whether the side-chain structure is modified and what effect that may have on the structural properties of the SCW (e.g. increasing wood flexibility and tolerance to mechanical perturbations). The relative reduction of xylan in tension wood and the increase in α-cellulose are consistent with the generally accepted model of physicochemical changes in tension wood, but do not agree with previous tension wood physicochemical characterizations of *E. globulus* that showed an increase in xylan and no change in cellulose (Aguayo *et al.*, 2010, 2012), although a reduction in lignin is consistently found.

Evidence for the increase in fibre cell formation in tension wood can be seen in the increase in the proportion of fibres (Table 1), which at a molecular level is evident in the up-regulation of methionine metabolism for ethylene production and GA and auxin signalling, as well as increased ontologies associated with programmed cell death (Tables 5, S6, Fig. S5). In terms of compositional changes in fibre SCW, the CAZymes observed to be up-regulated in tension wood-forming tissue (with the exception of GT8 and GT4) have been observed to be generally ubiquitously expressed across multiple tissues/organs of *E. grandis* or specific to primary cell wall tissues (Tables 4, S9). This observation could be attributable to the fact that tension wood produces increased amounts of carbohydrates generally not found in high abundance in *Eucalyptus* SCWs (such as galactose; Table 3, Fig. 2).

It is unclear in what form galacatose is present in the cell wall, as it could make up components of FLAs (Seifert & Roberts, 2007) or pectic compounds such as the side chains of rhamnogalacturonan I (Goubet *et al.*, 1995; Scheller *et al.*, 2007), or indeed be present as pure galactan. Nevertheless, the role of galactose and galactan in SCW and G-layer deposition, especially pertaining to orientation of cellulose microfibrils during cellulose deposition, has been previously highlighted (Gorshkova & Morvan, 2006; Roach *et al.*, 2011). Several studies have also reported the presence of β-(1→4) galactan and an increase in β-(1→6)

galactan in tension wood, some of unique composition not usually found in upright wood (Meier, 1962). We identified a homologue of the gene *AT3G27330*, encoding a protein of unknown function that has been annotated as possessing a GT92 domain (Yin *et al.*, 2012), also present in all three recently characterized GALACTAN SYNTHASE 1, 2 and 3 proteins, which were sufficient to increase cell wall galactan content (Liwanag *et al.*, 2012). This gene is not normally expressed in *Eucalyptus* xylem (Table S5), but is up-regulated in tension wood (Table 4), and would be a candidate for tension wood-specific β-(1→4) galactan synthesis.

The relative changes in cellulose quantity and properties are more complex, but are probably related to an increased carbon flux to UDP-glucose via SUSY, and/or a possible post-transcriptional/post-translational mechanism(s) that was not apparent in this study. The reduction in lignin can be attributed to a significant reduction in the expression of the suite of monolignol biosynthetic genes (Fig. 3, Table S7), as well as those involved in shikimate biosynthesis (*Eucgr.H01214*) and phenylalanine metabolism (*Eucgr.J00428*; Table S5). Together with enriched ontologies represented by up-regulated genes, it is our conclusion that, at a transcriptional level, the underlying molecular mechanism controlling *Eucalyptus* tension wood physiology is probably a reduction in lignin monomer production and xylan biosynthesis, and synthesis of polysaccharides not usually occurring in wood, rather than the relative up-regulation of pathways involved in secondary cell wall cellulose synthesis, as previously described.

Taken together, the findings of differentially expressed CAZymes provide new insight into changes in fibre cell wall size and composition in *Eucalyptus* tension wood. Recently, the function of PECTIN ACETYL ESTERASE 8 (PAE*8, E. grandis* homologue *Eucgr.E01169*) has been identified as deacetylating RG I in *A. thaliana* (de Souza *et al.*, 2014). Based on the differential GT and GH expression, and the wall changes in mannose and galactose, it is conceivable that during tension wood formation glucomannan is reduced by the shunting of mannose towards galactose production via GME. Galactose is incorporated into β-(1→4) galactan (both GT92- and GT32-containing genes up-regulated in *Eucalyptus* would be candidates for this; Table 4), and is probably incorporated into the wall as RG I in conjunction with FLA12. A modification of acetylation of RG I by PAE8 could theoretically decrease hydrophobicity and increase access to enzymatic breakdown (Busse-Wicher *et al.*, 2014; de Souza *et al.*, 2014) by, for example, β-galactosidases for cell wall remodelling (Roach *et al.*, 2011). Further reduction of glucomannan in the wall would occur via reduction of glucomannan synthase (although not detected as significant, the transcript level of the *E. grandis* homologue of *CELLULOSE SYNTHASE LIKE A 9* (*CSLA9*), *Eucgr.A01558*, was reduced by *c.* 4-fold in tension wood across all biological replicates; Table S5). Finally, although this should be tested in *Eucalyptus* in the future, the relative increase in cell wall deposition could be partially attributed to down-regulation of *MAN6* (*Eucgr.A00780*; Table 4). Suppression of the extracellular endo-1,4-β-mannanase MAN6 has been shown to increase SCW deposition in *Populus* by reducing mannose oligosaccharide signalling from the wall (Zhao *et al.*, 2013).

An aspect that still is not fully resolved, however, is the composition and interactions of matrix polysaccharides and the mechanism of tension generation. For example, the role of xyloglucan has been previously highlighted as playing a key role in generation of tension stress, with Xyloglucan endotransglucosylase/hydrolase (XET/XTH) enzymes providing the necessary active remodelling of interactions with crystalline cellulose (reviewed in Mellerowicz *et al.*, 2008; Mellerowicz & Gorshkova, 2012). Contrary to several previous tension wood studies, we observed no significant differential expression for any of the *c.* 40 annotated XET/XTH *E. grandis* homologues at 3 wk post induction in field-grown trees. Data generated in this study are more supportive of the paradigm where a change in the cellulose microfibril angle combined with a more hygroscopic cell wall composition would generate the tension necessary to oppose mechanical stress. In this paradigm, there is a decrease in MFA and shortening of the fibres in the case of angiosperms to generate tension at the top (Burgert & Fratzl, 2009), or an increase in MFA to lengthen fibres in compression wood at the bottom as observed in coniferous gymnosperms (Burgert *et al.*, 2007). This de-emphasizes specific architecture of the matrix polysaccharides but places greater emphasis on the orientation of cellulose fibrils, the chemical composition of the matrix and the resulting deformation allowable by relative matrix shear. Although it should not be discounted (fibre/tracheid cell length is still a critical factor of all types of reaction wood and XTHs play an important role in influencing primary elongation of fibres), the proposed role of XTHs in generating tension remains to be proven. Nevertheless, up-regulation of *XTH* genes has been demonstrated before in *Eucalyptus* during early tension wood formation (Paux *et al.*, 2005; Goulao *et al.*, 2011). The relative importance of active generation of tension by remodelling via hydolases (xyloglucan or galactose), as opposed to shrinking by matrix deformation, is still not resolved, and could be related to the type or developmental stage of tension wood formation.

Part of the novelty of this study is the fact that both physicochemical analyses and gene expression analyses were performed in field-grown trees. On the one hand, this introduces large biological variation and noise attributable to other environmental stressors such as interaction with pests and pathogens, and variability in light and temperature conditions that would not be found under laboratory conditions. Perhaps of most relevance to this study, these clonal stands are subject to constant coastal winds and especially young upright trees are constantly reacting to mechanical stress. This would create either microscopic regions of tension wood along the stem or, if evenly spread out, contribute to the overall low MFA and high crystallinity of cellulose observed in eucalypts. On the other hand, despite this variation, responses involving reduction of lignin, xylan and mannan, both in the wood chemistry and the molecular responses observed, were comparable with previous laboratory studies of tension wood formation. The results observed herein could be argued to be the most realistic biological response to mechanical stress in the field, over and above the normal wind and gravitational stresses experienced by a growing tree.

Eucalyptus is a commercially important hardwood genus, and the forest products industry will in the future undoubtedly rely on more sophisticated biotechnology strategies to enhance woody biomass traits. These strategies depend on understanding the roles of genes and biological processes during xylogenesis, including those involved in hormonal changes, cellular patterning, carbohydrate composition and cell wall ultrastructure. In this study, we have shown that gene expression and wood property changes during tension wood formation in field-grown *Eucalyptus* trees are to an extent consistent with previous results from model systems, highlighting key pathways and genes putatively involved in *Eucalyptus* tension wood formation specifically. Detailed microstructural studies will be needed to resolve any novel tension wood-specific polysaccharides or glycoprotein modifications, but this study suggests that the deposition of galactans not normally associated with secondary cell walls may play a role in tension wood formation or function in *Eucalyptus*. In the future, strategies to modify wood cell wall composition or ultrastructure in eucalypts will probably involve attenuation or overexpression of key genes, but could also involve the integration of novel biopolymers not normally found in wood.

Acknowledgements

The authors would like to acknowledge M. Ranik and M. O'Neill (University of Pretoria) for the mRNA-seq library preparations and the sequencing facility at Oregon State University for assistance with RNA sequencing. Plant material was kindly provided by Sappi Forest Research (KwaMbonambi, South Africa). This work was supported through a strategic research grant from the South African Department of Science and Technology (DST) and by research funding from Sappi and Mondi, through the Forest Molecular Genetics Programme, the Technology and Human Resources for Industry Programme (THRIP, UID 80118) and the Bioinformatics and Functional Genomics Programme of the National Research Foundation (NRF, UID 18312) of South Africa.

References

Abràmoff MD, Magalhães PJ, Ram SJ. 2004. Image processing with ImageJ. *Biophotonics International* **11**: 36–42.

Aguayo MG, Mendonça RT, Martínez P, Rodríguez J, Pereira M. 2012. Chemical characteristics and Kraft pulping of tension wood from *Eucalyptus globulus* Labill. *Revista Árvore* **36**: 1163–1172.

Aguayo MG, Quintupill L, Castillo R, Baeza J, Freer J, Mendonça RT. 2010. Determination of differences in anatomical and chemical characteristics of tension and opposite wood of 8-year old *Eucalyptus globulus*. *Maderas: Ciencia y Tecnologia* **12**: 241–251.

Al-Haddad JM, Kang K-Y, Mansfield SD, Telewski FW. 2013. Chemical responses to modified lignin composition in tension wood of hybrid poplar (*Populus tremula* × *Populus alba*). *Tree Physiology* **33**: 365–373.

Andersson-Gunneråas S, Hellgren JM, Björklund S, Regan S, Moritz T, Sundberg B. 2003. Asymmetric expression of a poplar ACC oxidase controls ethylene production during gravitational induction of tension wood. *Plant Journal* **34**: 339–349.

Andersson-Gunneråas S, Mellerowicz EJ, Love J, Segerman B, Ohmiya Y, Coutinho PM, Nilsson P, Henrissat B, Moritz T, Sundberg B. 2006. Biosynthesis of cellulose-enriched tension wood in *Populus*: global analysis of transcripts and metabolites identifies biochemical and developmental regulators in secondary wall biosynthesis. *Plant Journal* **45**: 144–165.

Aoyama W, Matsumura A, Tsutsumi Y, Nishida T. 2001. Lignification and peroxidase in tension wood of *Eucalyptus viminalis* seedlings. *Journal of Wood Science* **47**: 419–424.

Auldridge ME, Block A, Vogel JT, Dabney-Smith C, Mila I, Bouzayen M, Magallanes-Lundback M, DellaPenna D, McCarty DR, Klee HJ. 2006. Characterization of three members of the *Arabidopsis* carotenoid cleavage dioxygenase family demonstrates the divergent roles of this multifunctional enzyme family. *Plant Journal* **45**: 982–993.

Baba K, Karlberg A, Schmidt J, Schrader J, Hvidsten TR, Bako L, Bhalerao RP. 2011. Activity-dormancy transition in the cambial meristem involves stage-specific modulation of auxin response in hybrid aspen. *Proceedings of the National Academy of Sciences, USA* **108**: 3418–3423.

Baba K, Park YW, Kaku T, Kaida R, Takeuchi M, Yoshida M, Hosoo Y, Ojio Y, Okuyama T, Taniguchi T *et al.* 2009. Xyloglucan for generating tensile stress to bend tree stem. *Molecular Plant* **2**: 893–903.

Bentum ALK, Côté WA Jr, Day AC, Timell TE. 1969. Distribution of lignin in normal and tension wood. *Wood Science and Technology* **3**: 218–231.

Björklund S, Antti H, Uddestrand I, Moritz T, Sundberg B. 2007. Cross-talk between gibberellin and auxin in development of *Populus* wood: gibberellin stimulates polar auxin transport and has a common transcriptome with auxin. *Plant Journal* **52**: 499–511.

Bowling AJ, Vaughn KC. 2008. Immunocytochemical characterization of tension wood: gelatinous fibers contain more than just cellulose. *American Journal of Botany* **95**: 655–663.

Browning B. 1967. *Methods of wood chemistry*. New York, NY, USA: Wiley Interscience.

Burgert I, Eder M, Gierlinger N, Fratzl P. 2007. Tensile and compressive stresses in tracheids are induced by swelling based on geometrical constraints of the wood cell. *Planta* **226**: 981–987.

Burgert I, Fratzl P. 2009. Plants control the properties and actuation of their organs through the orientation of cellulose fibrils in their cell walls. *Integrative and Comparative Biology* **49**: 69–79.

Busse-Wicher M, Gomes TC, Tryfona T, Nikolovski N, Stott K, Grantham NJ, Bolam DN, Skaf MS, Dupree P. 2014. The pattern of xylan acetylation suggests xylan may interact with cellulose microfibrils as a two-fold helical screw in the secondary plant cell wall of Arabidopsis thaliana. *Plant Journal* **79**: 492–506.

Caffall KH, Mohnen D. 2009. The structure, function, and biosynthesis of plant cell wall pectic polysaccharides. *Carbohydrate Research* **344**: 1879–1900.

Chang S, Puryear J, Cairney J. 1993. A simple and efficient method for isolating RNA from pine trees. *Plant Molecular Biology Reporter* **11**: 113–116.

Clair B, Alméras T, Pilate G, Jullien D, Sugiyama J, Riekel C. 2011. Maturation stress generation in poplar tension wood studied by synchrotron radiation microdiffraction. *Plant Physiology* **155**: 562–570.

Clair B, Alméras T, Yamamoto H, Okuyama T, Sugiyama J. 2006a. Mechanical behavior of cellulose microfibrils in tension wood, in relation with maturation stress generation. *Biophysical Journal* **91**: 1128–1135.

Clair B, Ruelle J, Beauchêne J, Prévost MF, Fournier M. 2006b. Tension wood and opposite wood in 21 tropical rain forest species. 1. Occurrence and efficiency of the G-layer.. *IAWA Journal* **27**: 329–338.

Coleman HD, Yan J, Mansfield SD. 2009. Sucrose synthase affects carbon partitioning to increase cellulose production and altered cell wall ultrastructure. *Proceedings of the National Academy of Sciences, USA* **106**: 13118–13123.

Côté WA Jr, Day AC, Timell TE. 1969. A contribution to the ultrastructure of tension wood fibers. *Wood Science and Technology* **3**: 257–271.

Elo A, Immanen J, Nieminen K, Helariutta Y. 2009. Stem cell function during plant vascular development. *Seminars in Cell and Developmental Biology* **20**: 1097–1106.

Falconer MM, Seagull RW. 1985. Immunofluorescent and calcofluor white staining of developing tracheary elements in *Zinnia elegans* L. suspension cultures. *Protoplasma* **125**: 190–198.

Fang CH, Clair B, Gril J, Alméras T. 2007. Transverse shrinkage in G-fibers as a function of cell wall layering and growth strain. *Wood Science and Technology* **41**: 659–671.

Fang CH, Clair B, Gril J, Liu SQ. 2008. Growth stresses are highly controlled by the amount of G-layer in poplar tension wood. *Iawa Journal* **29**: 237–246.
Gorshkova T, Morvan C. 2006. Secondary cell-wall assembly in flax phloem fibres: role of galactans. *Planta* **223**: 149–158.
Goswami L, Dunlop JWC, Jungnikl K, Eder M, Gierlinger N, Coutand C, Jeronimidis G, Fratzl P, Burgert I. 2008. Stress generation in the tension wood of poplar is based on the lateral swelling power of the G-layer. *Plant Journal* **56**: 531–538.
Goubet F, Bourlard T, Girault R, Alexandre C, Vandevelde MC, Morvan C. 1995. Structural features of galactans from flax fibres. *Carbohydrate Polymers* **27**: 221–227.
Goulao LF, Vieira-Silva S, Jackson PA. 2011. Association of hemicellulose- and pectin-modifying gene expression with *Eucalyptus globulus* secondary growth. *Plant Physiology and Biochemistry* **49**: 873–881.
Humphreys JM, Chapple C. 2002. Rewriting the lignin roadmap. *Current Opinion in Plant Biology* **5**: 224–229.
Jin H, Do J, Moon D, Noh EW, Kim W, Kwon M. 2011. EST analysis of functional genes associated with cell wall biosynthesis and modification in the secondary xylem of the yellow poplar (*Liriodendron tulipifera*) stem during early stage of tension wood formation. *Planta* **234**: 959–977.
Joseleau JP, Imai T, Kuroda K, Ruel K. 2004. Detection in situ and characterization of lignin in the G-layer of tension wood fibres of *Populus deltoides*. *Planta* **219**: 338–345.
Jourez B, Riboux A, Leclercq A. 2001. Anatomical characteristics of tension wood and opposite wood in young inclined stems of poplar (*Populus euramericana* cv 'Ghoy'). *IAWA Journal* **22**: 133–157.
Ko JH, Han KH, Park S, Yang J. 2004. Plant body weight-induced secondary growth in *Arabidopsis* and its transcription phenotype revealed by whole-transcriptome profiling. *Plant Physiology* **135**: 1069–1083.
Ko JH, Kim WC, Han KH. 2009. Ectopic expression of MYB46 identifies transcriptional regulatory genes involved in secondary wall biosynthesis in *Arabidopsis*. *Plant Journal* **60**: 649–665.
Lafarguette F, Leplé JC, Déjardin A, Laurans F, Costa G, Lesage-Descauses MC, Pilate G. 2004. Poplar genes encoding fasciclin-like arabinogalactan proteins are highly expressed in tension wood. *New Phytologist* **164**: 107–121.
Lee C, Teng Q, Zhong R, Ye ZH. 2012. *Arabidopsis* GUX proteins are glucuronyltransferases responsible for the addition of glucuronic acid side chains onto xylan. *Plant and Cell Physiology* **53**: 1204–1216.
Leinonen R, Sugawara H, Shumway M. 2010. The sequence read archive. *Nucleic Acids Research* **39**: D19–D21.
Little CHA, Savidge RA. 1987. 7. The role of plant growth regulators in forest tree cambial growth. *Plant Growth Regulation* **6**: 137–169.
Liwanag AJM, Ebert B, Verhertbruggen Y, Rennie EA, Rautengarten C, Oikawa A, Andersen MC, Clausen MH, Scheller HV. 2012. Pectin biosynthesis: GALS1 in *Arabidopsis thaliana* is a β-1, 4-galactan β-1, 4-galactosyltransferase. *The Plant Cell Online* **24**: 5024–5036.
Lloyd C. 2011. Dynamic microtubules and the texture of plant cell walls. *International Review of Cell and Molecular Biology* **287**: 287–329.
Love J, Björklund S, Vahala J, Hertzberg M, Kangasjärvi J, Sundberg B. 2009. Ethylene is an endogenous stimulator of cell division in the cambial meristem of *Populus*. *Proceedings of the National Academy of Sciences, USA* **106**: 5984–5989.
Maere S, Heymans K, Kuiper M. 2005. BiNGO: a Cytoscape plugin to assess overrepresentation of Gene Ontology categories in biological networks. *Bioinformatics* **21**: 3448–3449.
Major LL, Wolucka BA, Naismith JH. 2005. Structure and function of GDP-mannose-3′,5′-epimerase: an enzyme which performs three chemical reactions at the same active site. *Journal of the American Chemical Society* **127**: 18309–18320.
Martin D, Brun C, Remy E, Mouren P, Thieffry D, Jacq B. 2004. GOToolBox: functional analysis of gene datasets based on Gene Ontology. *Genome Biology* **5**: R101.
Meier H. 1962. Studies on a galactan from tension wood of beech (*Fagus silvatica* L.). *Acta Chemica Scandinavica* **16**: 14.
Mellerowicz EJ, Gorshkova TA. 2012. Tensional stress generation in gelatinous fibres: a review and possible mechanism based on cell-wall structure and composition. *Journal of Experimental Botany* **63**: 551–565.
Mellerowicz EJ, Immerzeel P, Hayashi T. 2008. Xyloglucan: the molecular muscle of trees. *Annals of Botany* **102**: 659–665.
Mortimer JC, Miles GP, Brown DM, Zhang Z, Segura MP, Weimar T, Yu X, Seffen KA, Stephens E, Turner SR *et al.* 2010. Absence of branches from xylan in *Arabidopsis* gux mutants reveals potential for simplification of lignocellulosic biomass. *Proceedings of the National Academy of Sciences, USA* **107**: 17409–17414.
Moyle R, Schrader J, Stenberg A, Olsson O, Saxena S, Sandberg G, Bhalerao RP. 2002. Environmental and auxin regulation of wood formation involves members of the Aux/IAA gene family in hybrid aspen. *Plant Journal* **31**: 675–685.
Muller M, Burghammer M, Sugiyama J. 2006. Direct investigation of the structural properties of tension wood cellulose microfibrils using microbeam X-ray fibre diffraction. *Holzforschung* **60**: 474–479.
Myburg AA, Grattapaglia D, Tuskan GA, Hellsten U, Hayes RD, Grimwood J, Jenkins J, Lindquist E, Tice H, Bauer D *et al.* 2014. The genome of *Eucalyptus grandis*. *Nature* **510**: 356–362.
Nishikubo N, Awano T, Banasiak A, Bourquin V, Ibatullin F, Funada R, Brumer H, Teeri TT, Hayashi T, Sundberg B *et al.* 2007. Xyloglucan endo-transglycosylase (XET) functions in gelatinous layers of tension wood fibers in poplar – a glimpse into the mechanism of the balancing act of trees. *Plant and Cell Physiology* **48**: 843–855.
Okuyama T, Yamamoto H, Yoshida M, Hattori Y, Archer RR. 1994. Growth stresses in tension wood: role of microfibrils and lignification. *Annales des Sciences Forestieres* **51**: 291–300.
Paux E, Carocha V, Marques C, De Sousa AM, Borralho N, Sivadon P, Grima-Pettenati J. 2005. Transcript profiling of *Eucalyptus* xylem genes during tension wood formation. *New Phytologist* **167**: 89–100.
Pesquet E, Tuominen H. 2011. Ethylene stimulates tracheary element differentiation in *Zinnia elegans* cell cultures. *New Phytologist* **190**: 138–149.
Qiu D, Wilson IW, Gan S, Washusen R, Moran GF, Southerton SG. 2008. Gene expression in *Eucalyptus* branch wood with marked variation in cellulose microfibril orientation and lacking G-layers. *New Phytologist* **179**: 94–103.
Ranik M, Myburg AA. 2006. Six new cellulose synthase genes from *Eucalyptus* are associated with primary and secondary cell wall biosynthesis. *Tree Physiology* **26**: 545–556.
Roach MJ, Mokshina NY, Badhan A, Snegireva AV, Hobson N, Deyholos MK, Gorshkova TA. 2011. Development of cellulosic secondary walls in flax fibers requires β-galactosidase. *Plant Physiology* **156**: 1351–1363.
Romano JM, Dubos C, Prouse MB, Wilkins O, Hong H, Poole M, Kang KY, Li E, Douglas CJ, Western TL. 2012. AtMYB61, an R2R3-MYB transcription factor, functions as a pleiotropic regulator via a small gene network. *New Phytologist* **195**: 774–786.
Ruelle J, Beauchêne J, Yamamoto H, Thibaut B. 2010. Variations in physical and mechanical properties between tension and opposite wood from three tropical rainforest species. *Wood Science and Technology* **45**: 339–537.
Ruelle J, Clair B, Beauchêne J, Prévost MF, Fournier M. 2006. Tension wood and opposite wood in 21 tropical rain forest species 2. Comparison of some anatomical and ultrastructural criteria. *IAWA Journal* **27**: 341–376.
Scheller HV, Jensen JK, Sørensen SO, Harholt J, Geshi N. 2007. Biosynthesis of pectin. *Physiologia Plantarum* **129**: 283–295.
Schroeder A, Mueller O, Stocker S, Salowsky R, Leiber M, Gassmann M, Lightfoot S, Menzel W, Granzow M, Ragg T. 2006. The RIN: an RNA integrity number for assigning integrity values to RNA measurements. *BMC Molecular Biology* **7**: 3.
Sehr EM, Agusti J, Lehner R, Farmer EE, Schwarz M, Greb T. 2010. Analysis of secondary growth in the *Arabidopsis* shoot reveals a positive role of jasmonate signalling in cambium formation. *Plant Journal* **63**: 811–822.
Seifert GJ, Roberts K. 2007. The biology of arabinogalactan proteins. *Annual Review of Plant Biology* **58**: 137–161.
Smirnoff N. 2011. Vitamin C: the metabolism and functions of ascorbic acid in plants. *Advances in Botanical Research* **59**: 107–177.

de Souza A, Hull PA, Gille S, Pauly M. 2014. Identification and functional characterization of the distinct plant pectin esterases PAE8 and PAE9 and their deletion mutants. *Planta* **240**: 1123–1138.

Trapnell C, Pachter L, Salzberg SL. 2009. TopHat: discovering splice junctions with RNA-Seq. *Bioinformatics* **25**: 1105–1111.

Trapnell C, Williams BA, Pertea G, Mortazavi A, Kwan G, van Baren MJ, Salzberg SL, Wold BJ, Pachter L. 2010. Transcript assembly and quantification by RNA-Seq reveals unannotated transcripts and isoform switching during cell differentiation. *Nature Biotechnology* **28**: 511–515.

Ukrainetz NK, Kang K-Y, Aitken SN, Stoehr M, Mansfield SD. 2008. Heritability and phenotypic and genetic correlations of coastal Douglas-fir (*Pseudotsuga menziesii*) wood quality traits. *Canadian Journal of Forest Research* **38**: 1536–1546.

Vahala J, Felten J, Love J, Gorzsas A, Gerber L, Lamminmaki A, Kangasjarvi J, Sundberg B. 2013. A genome-wide screen for ethylene-induced ethylene response factors (ERFs) in hybrid aspen stem identifies ERF genes that modify stem growth and wood properties. *New Phytologist* **200**: 511–522.

Washusen R, Evans R, Southerton S. 2005. A study of *Eucalyptus grandis* and *Eucalyptus globulus* branch wood microstructure. *Iawa Journal* **26**: 203–210.

Washusen R, Ilic J, Waugh G. 2003. The relationship between longitudinal growth strain, tree form and tension wood at the stem periphery of ten- to eleven-year-old *Eucalyptus globulus* labill. *Holzforschung* **57**: 308–316.

Wolucka BA, Van Montagu M. 2003. GDP-Mannose 3′,5′-Epimerase forms GDP-L-gulose, a putative intermediate for the *de novo* biosynthesis of vitamin C in plants. *Journal of Biological Chemistry* **278**: 47483–47490.

Yamamoto H. 2004. Role of the gelatinous layer on the origin of the physical properties of the tension wood. *Journal of Wood Science* **50**: 197–208.

Yin Y, Mao X, Yang J, Chen X, Mao F, Xu Y. 2012. DbCAN: a web resource for automated carbohydrate-active enzyme annotation. *Nucleic Acids Research* **40** (W1): W445–W451.

Yokoyama T, Kadla J, Chang H. 2002. Microanalytical method for the characterization of fiber components and morphology of woody plants. *Journal of Agricultural and Food Chemistry* **50**: 1040–1044.

Yoshida M, Ohta H, Yamamoto H, Okuyama T. 2002. Tensile growth stress and lignin distribution in the cell walls of yellow poplar, *Liriodendron tulipifera* Linn. *Trees – Structure and Function* **16**: 457–464.

Yoshizawa N, Inami A, Miyake S, Ishiguri F, Yokota S. 2000. Anatomy and lignin distribution of reaction wood in two *Magnolia* species. *Wood Science and Technology* **34**: 183–196.

Zhao Y, Song D, Sun J, Li L. 2013. Populus endo-beta-mannanase PtrMAN6 plays a role in coordinating cell wall remodeling with suppression of secondary wall thickening through generation of oligosaccharide signals. *Plant Journal* **74**: 473–485.

Fig. S1 Trees used for analysis of physicochemical changes in tension wood properties. Five individuals (ramets) of a commercial hybrid *Eucalyptus grandis* × *E. urophylla* F_1 hybrid clone (GUSAP1) were selected with naturally slanting branches emerging from the base of the tree. A transverse disc (bottom left) was cut from an area of the branch which was at approximately 45° from the longitudinal axis of the tree trunk. TW, tension wood; OW, opposite wood.

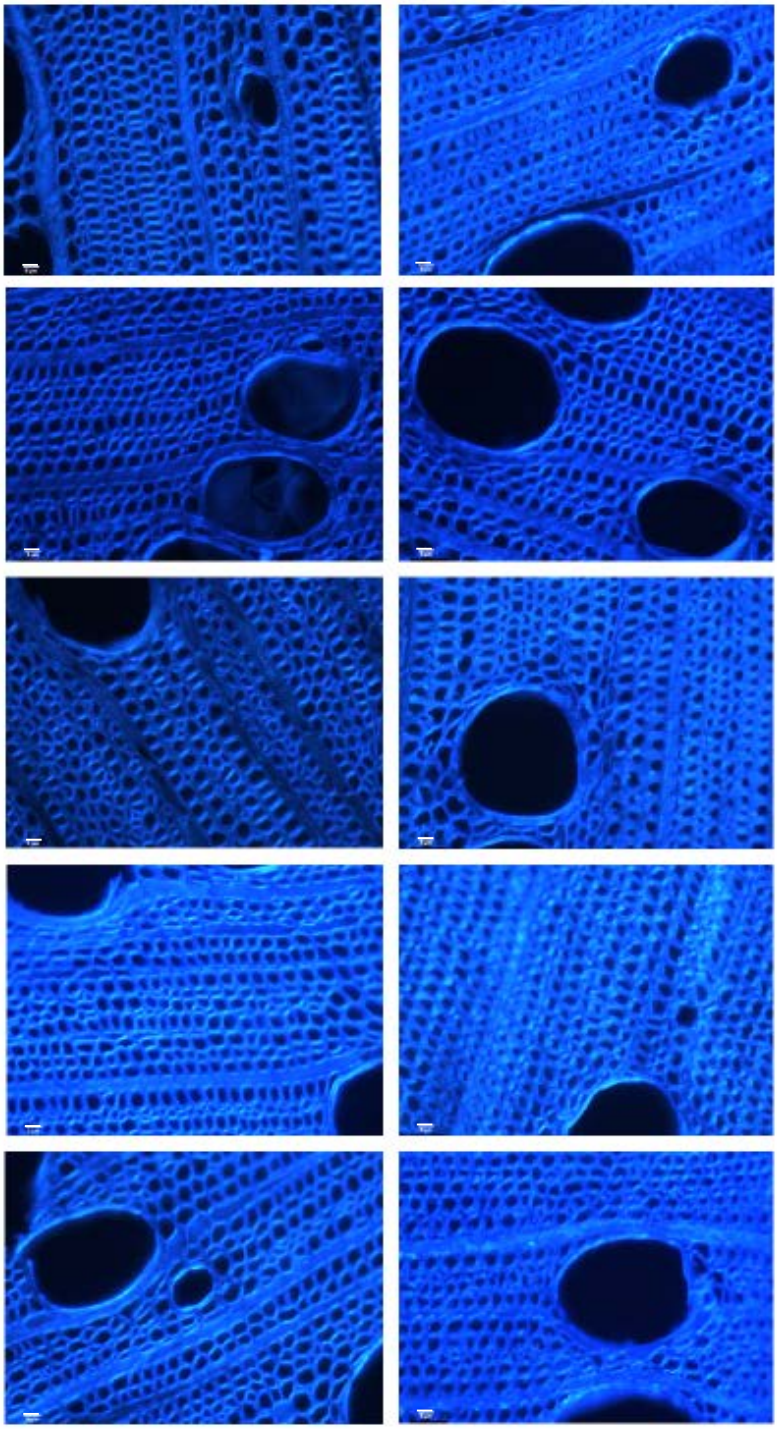

Fig. S2 Comparison of opposite wood (left) and tension wood (right) tissue from five ramets (top to bottom, 1–5 from Supporting Information Fig. S1) of an F_1 hybrid clone of *Eucalyptus grandis* and *E. urophylla* (GUSAP1). Bar, 5 µm.

Fig. S3 Cross section of the main stem of an 18-month-old GUSAP1 (*E. grandis* × *E. urophylla*) tree after 6 months of bending. Tension wood can be seen at a macroscopic level on the top half of the bent trunk.

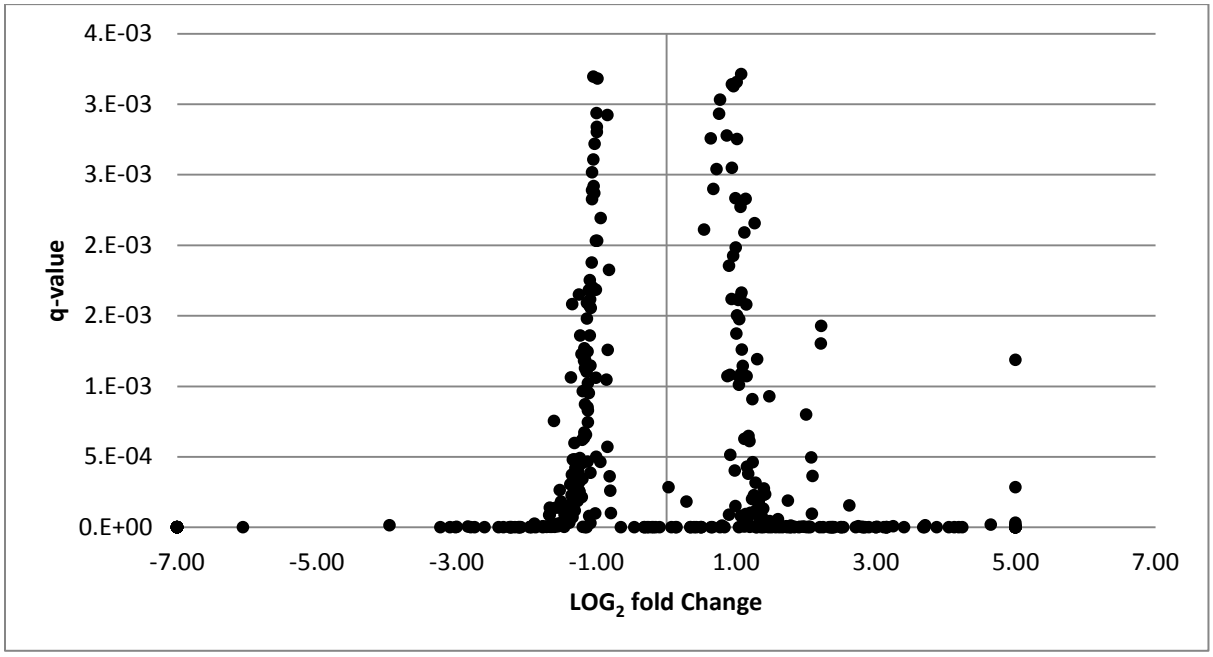

Fig. S4 Volcano plot of significantly differentially expressed genes in 3-wk tension wood vs upright control.

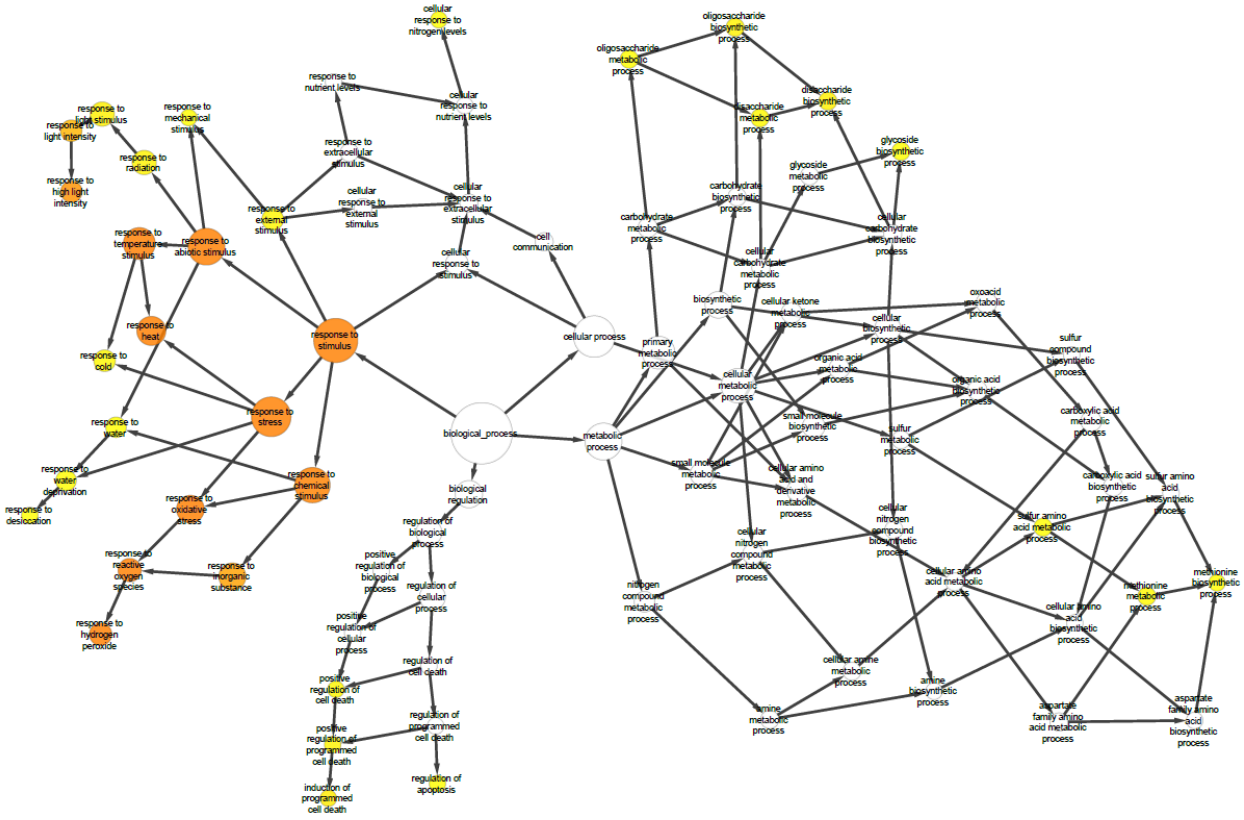

Fig. S5 Significantly enriched gene ontology (GO) terms in differentially upregulated genes in induced tension wood xylem compared with upright control xylem.

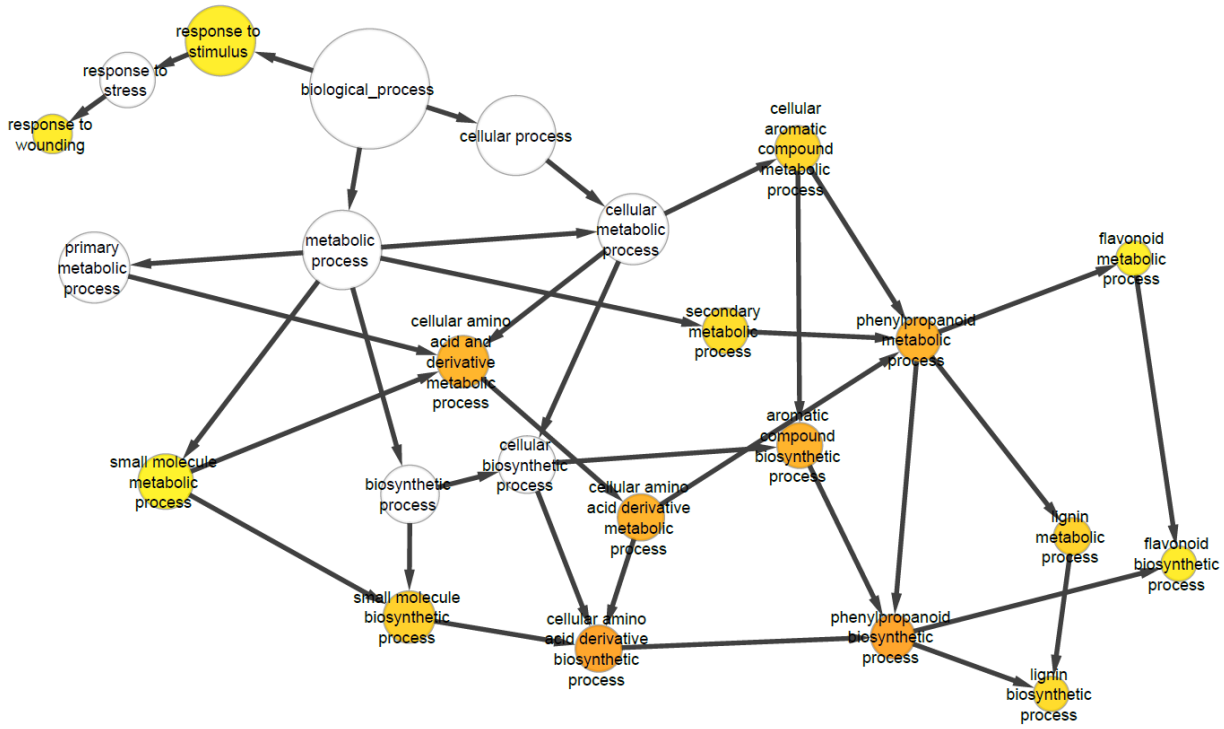

Fig. S6 Significantly enriched gene ontology (GO) terms in differentially downregulated genes in induced tension wood xylem compared with upright control xylem.

Fig. S7 Evidence for tension wood-specific expression of a tandem gene copy of a secondary cell wall cellulose synthase gene. The genomic region of the paralogous cellulose synthase gene expressed in tension wood (top) and not in the upright control (bottom) is highlighted in the red box. The sequence of this paralog was interrogated and predicts a full length in-frame duplicate of EgCesA3, as annotated by Ranik & Myburg, 2006.

Ranik M, Myburg AA. 2006. Six new cellulose synthase genes from *Eucalyptus* are associated with primary and secondary cell wall biosynthesis. *Tree Physiology* **26:** 545–556.

Table S1 Numbers of mRNA-seq reads mapping to *Eucalyptus grandis* genome

Tissue type	**Sample ID**	**Mapped reads**
Tensionwood	tensionwood1	8,779,533
Tensionwood	tensionwood2	8,099,046
Tensionwood	tensionwood3	9,830,430
Xylem	upright1	19,053,227
Xylem	upright2	19,876,244
Xylem	upright3	12,368,913

Table S2 Summary of relative changes in microfibril angle (MFA), lignin, and cell wall sugars in tension wood compared with opposite wood in five trees

Tree	Δ MFA in TW	Δ% Insoluble lignin	Δ% Lignin	ΔGalactose	ΔGlucose	ΔXylose	ΔMannose
1	8.91%	0.04%	0.46%	170.37%	13.70%	-16.43%	-34.47%
2	-7.25%	-6.71%	-5.53%	151.83%	16.16%	-17.02%	-26.44%
3	-13.96%	-4.85%	-4.43%	198.28%	14.84%	-22.13%	-46.86%
4	-10.19%	-3.36%	-2.80%	298.24%	9.16%	-26.64%	-40.70%
5	-2.63%	-6.83%	-6.75%	267.49%	27.70%	-10.26%	-31.12%
MEAN	**-5.02%**	**-4.34%**	**-3.81%**	**217.24%**	**16.31%**	**-18.50%**	**-35.92%**
SD	8.82%	2.84%	2.79%	63.09%	6.89%	6.20%	8.02%
SE	3.95%	1.27%	1.25%	28.21%	3.08%	2.77%	3.59%

TW, tension wood.

Table S3 Relative changes in holocellulose, α-cellulose and total glucose in tension wood compared with opposite wood in five trees

Tree	**Δ% Holocellulose**	**Δ% α-cellulose**	**Δ%Glucose**
1	-0.02%	9.32%	13.70%
2	-1.73%	1.79%	16.16%
3	2.16%	12.44%	14.84%
4	6.71%	6.09%	9.16%
5	7.26%	-0.82%	27.70%
MEAN	**2.87%**	**5.77%**	**16.31%**
SD	4.00%	5.39%	6.89%
SE	1.79%	2.41%	3.08%

Table S6 GoToolBox analysis of 3 wk TW differentially expressed genes.

Upregulated – BP

GO_ID	Level(s)	Term	*P*-value	Enrichment (E)/depletion (D)
GO:0009408	5,4	**response to heat**	2.67E-22	E
GO:0009266	4	**response to temperature stimulus**	2.03E-20	E
GO:0009628	3	**response to abiotic stimulus**	4.20E-18	E
GO:0050896	2	**response to stimulus**	3.08E-16	E
GO:0006950	3	**response to stress**	4.73E-15	E
GO:0000302	5	**response to reactive oxygen species**	2.38E-12	E
GO:0042542	6	**response to hydrogen peroxide**	1.42E-11	E
GO:0006979	4	**response to oxidative stress**	1.42E-11	E
GO:0009644	7	**response to high light intensity**	2.83E-09	E
GO:0042221	3	**response to chemical stimulus**	6.29E-09	E
GO:0009642	6	**response to light intensity**	7.58E-08	E
GO:0009416	5	**response to light stimulus**	8.57E-06	E
GO:0009314	4	**response to radiation**	1.08E-05	E
GO:0009409	5,4	**response to cold**	5.44E-05	E
GO:0009725	4	**response to hormone stimulus**	8.19E-05	E
GO:0012502	8,6,7	**induction of programmed cell death**	1.13E-04	E
GO:0043068	7,5,6	**positive regulation of programmed cell death**	1.57E-04	E

GO:0009719	3	**response to endogenous stimulus**	1.58E-04	E
GO:0010942	6,4,5	**positive regulation of cell death**	2.09E-04	E
GO:0046351	6,7	**disaccharide biosynthetic process**	3.35E-04	E
GO:0005984	5,6	**disaccharide metabolic process**	6.95E-04	E
GO:0009612	4	**response to mechanical stimulus**	8.76E-04	E
GO:0032502	2	**developmental process**	8.98E-04	E
GO:0042981	7,6	**regulation of apoptosis**	9.90E-04	E
GO:0009414	5,4	**response to water deprivation**	1.05E-03	E
GO:0009269	6,5	**response to desiccation**	1.24E-03	E
GO:0009415	4	**response to water**	1.40E-03	E
GO:0032501	2	**multicellular organismal process**	1.47E-03	E
GO:0009605	3	**response to external stimulus**	2.30E-03	E
GO:0007638	4,5	**mechanosensory behavior**	2.77E-03	E
GO:0010032	5,6	**meiotic chromosome condensation**	2.77E-03	E
GO:0005992	7,8	**trehalose biosynthetic process**	3.26E-03	E
GO:0043067	6,5	**regulation of programmed cell death**	3.26E-03	E
GO:0010941	5,4	**regulation of cell death**	3.47E-03	E
GO:0005991	6,7	**trehalose**	3.90E-03	E

		metabolic process		
GO:0007017	3	**microtubule-based process**	4.60E-03	E
GO:0051707	3,4	**response to other organism**	4.75E-03	E
GO:0007169	8,7	**transmembrane receptor protein tyrosine kinase signaling pathway**	5.22E-03	E
GO:0007167	7,6	**enzyme linked receptor protein signaling pathway**	5.22E-03	E
GO:0051316	10,9,5,8,4,7,6	**attachment of spindle microtubules to kinetochore during meiotic chromosome segregation**	5.52E-03	E
GO:0008608	9,8,5,7	**attachment of spindle microtubules to kinetochore**	5.52E-03	E
GO:0045143	10,8,7,5,9,6,4	**homologous chromosome segregation**	5.52E-03	E
GO:0051313	8,7,4,6	**attachment of spindle microtubules to chromosome**	5.52E-03	E
GO:0051754	7,11,9,5,10,8,4,6	**meiotic sister chromatid cohesion, centromeric**	5.52E-03	E
GO:0051455	11,10,6,9,8,5,7	**attachment of spindle microtubules to kinetochore during meiosis I**	5.52E-03	E
GO:0034453	7,6,5	**microtubule anchoring**	5.52E-03	E
GO:0000226	5,4	**microtubule cytoskeleton**	5.86E-03	E

		organization		
GO:0048856	3	**anatomical structure development**	5.87E-03	E
GO:0009607	3	**response to biotic stimulus**	6.79E-03	E
GO:0009737	5	**response to abscisic acid stimulus**	6.85E-03	E
GO:0008219	3	**cell death**	6.93E-03	E
GO:0016265	2	**death**	6.93E-03	E
GO:0009804	5,4	**coumarin metabolic process**	8.26E-03	E
GO:0009805	6,5	**coumarin biosynthetic process**	8.26E-03	E
GO:0006555	7,8,6	**methionine metabolic process**	8.78E-03	E
GO:0051094	5,3,4	**positive regulation of developmental process**	9.10E-03	E
GO:0007166	6,5	**cell surface receptor linked signal transduction**	9.17E-03	E
GO:0042446	6,4	**hormone biosynthetic process**	9.75E-03	E
GO:0034754	6,4	**cellular hormone metabolic process**	9.75E-03	E
GO:0034961	6	**cellular biopolymer biosynthetic process**	6.97E-03	D
GO:0043284	5	**biopolymer biosynthetic process**	6.73E-03	D
GO:0010467	4	**gene expression**	3.30E-03	D

Upregulated – MF

GO_ID	Level(s)	Term	*P*-value	Enrichment (E)/depletion (D)
GO:0016684	4	**oxidoreductase activity, acting on peroxide as acceptor**	5.76E-06	E
GO:0004601	3,5	**peroxidase activity**	5.76E-06	E
GO:0016209	2	**antioxidant activity**	1.06E-05	E
GO:0016491	3	**oxidoreductase activity**	5.14E-05	E
GO:0004805	8	**trehalose-phosphatase activity**	6.22E-04	E
GO:0019203	7	**carbohydrate phosphatase activity**	8.81E-04	E
GO:0005200	3	**structural constituent of cytoskeleton**	2.18E-03	E
GO:0046409	5	**p-coumarate 3-hydroxylase activity**	2.33E-03	E
GO:0043864	6	**indoleacetamide hydrolase activity**	2.33E-03	E
GO:0010349	6	**L-galactose dehydrogenase activity**	2.33E-03	E
GO:0008379	5,7	**thioredoxin peroxidase activity**	2.33E-03	E
GO:0005372	4	**water transporter activity**	3.29E-03	E
GO:0015250	5,7	**water channel activity**	3.29E-03	E
GO:0004679	8	**AMP-activated protein kinase activity**	4.64E-03	E
GO:0008705	7	**methionine synthase activity**	6.95E-03	E
GO:0003871	7	**5-methyltetrahydropteroyltriglutamate-homocysteine S-methyltransferase activity**	6.95E-03	E
GO:0080064	7	**4,4-dimethyl-9beta,19-cyclopropylsterol-4alpha-methyl oxidase activity**	6.95E-03	E
GO:0004096	4,6	**catalase activity**	6.95E-03	E
GO:0042085	6	**5-methyltetrahydropteroyltri-L-glutamate-dependent methyltransferase activity**	6.95E-03	E
GO:0042084	6	**5-methyltetrahydrofolate-dependent methyltransferase activity**	6.95E-03	E

GO:0016757	4	**transferase activity, transferring glycosyl groups**	7.00E-03	E
GO:0010309	6	**acireductone dioxygenase [iron(II)-requiring] activity**	9.24E-03	E
GO:0004645	6	**phosphorylase activity**	9.24E-03	E
GO:0051920	4,6	**peroxiredoxin activity**	9.24E-03	E
GO:0003824	2	**catalytic activity**	9.57E-03	E

Upregulated – CC

GO_ID	Level(s)	Term	*P*-value	Enrichment (E)/depletion (D)
GO:0045298	10,9,8,7,6,4,5	**tubulin complex**	2.04E-04	E
GO:0005829	8,7,6,5	**cytosol**	7.13E-04	E
GO:0005792	8,7	**microsome**	9.82E-04	E
GO:0042598	7,6	**vesicular fraction**	9.82E-04	E
GO:0005737	6,5,4	**cytoplasm**	1.00E-03	E
GO:0005626	5,4	**insoluble fraction**	1.39E-03	E
GO:0005624	6,5	**membrane fraction**	1.39E-03	E
GO:0005874	10,9,8,7,6,5	**microtubule**	1.48E-03	E
GO:0010319	11,10,9,8,7,6,5	**stromule**	1.77E-03	E
GO:0000267	4,3	**cell fraction**	1.87E-03	E
GO:0044444	7,6,5,4	**cytoplasmic part**	2.17E-03	E
GO:0044424	5,4,3	**intracellular part**	2.19E-03	E
GO:0005622	4,3	**intracellular**	2.30E-03	E
GO:0044430	9,8,7,6,5,4	**cytoskeletal part**	3.80E-03	E
GO:0005856	8,7,6,5	**cytoskeleton**	5.68E-03	E
GO:0048196	5,4	**middle lamella-containing extracellular matrix**	7.12E-03	E
GO:0005876	11,9,10,8,7,6	**spindle microtubule**	8.88E-03	E
GO:0008278	10,9,8,7,6,4,5	**cohesin complex**	8.88E-03	E
GO:0012505	4,3	**endomembrane system**	1.82E-03	D

Downregulated - BP

GO_ID	Level(s)	Term	*P*-value	Enrichment (E)/depletion (D)
GO:0042398	6,5	**cellular amino acid derivative biosynthetic process**	5.59E-11	E
GO:0009699	7,6,5	**phenylpropanoid biosynthetic process**	5.69E-10	E
GO:0006575	5	**cellular amino acid derivative metabolic process**	1.14E-09	E
GO:0019438	5	**aromatic compound biosynthetic process**	1.86E-09	E
GO:0009698	6,5,4	**phenylpropanoid metabolic process**	5.04E-09	E
GO:0006519	4	**cellular amino acid and derivative metabolic process**	5.44E-09	E
GO:0006725	4	**cellular aromatic compound metabolic process**	5.56E-07	E
GO:0009611	4	**response to wounding**	7.64E-07	E
GO:0019748	3	**secondary metabolic process**	9.69E-07	E
GO:0009809	8,7,6	**lignin biosynthetic process**	6.65E-06	E
GO:0009605	3	**response to external stimulus**	2.07E-05	E
GO:0009808	7,6,5	**lignin metabolic process**	2.90E-05	E
GO:0050896	2	**response to stimulus**	3.59E-05	E
GO:0009813	8,7,6	**flavonoid biosynthetic process**	7.37E-05	E
GO:0009812	7,6,5	**flavonoid metabolic process**	1.15E-04	E
GO:0009416	5	**response to light stimulus**	2.42E-04	E
GO:0009628	3	**response to abiotic stimulus**	2.55E-04	E
GO:0009314	4	**response to radiation**	2.93E-04	E
GO:0006949	4,3,6,5	**syncytium formation**	4.99E-04	E

GO:0006807	3	**nitrogen compound metabolic process**	7.04E-04	E
GO:0009719	3	**response to endogenous stimulus**	7.46E-04	E
GO:0009411	6	**response to UV**	1.24E-03	E
GO:0034641	4	**cellular nitrogen compound metabolic process**	1.99E-03	E
GO:0042221	3	**response to chemical stimulus**	2.98E-03	E
GO:0042180	4	**cellular ketone metabolic process**	3.39E-03	E
GO:0009714	7,6,5	**chalcone metabolic process**	3.39E-03	E
GO:0000072	7,6,4	**M phase specific microtubule process**	3.39E-03	E
GO:0009715	8,7,6	**chalcone biosynthetic process**	3.39E-03	E
GO:0019695	8	**choline metabolic process**	3.39E-03	E
GO:0042181	5	**ketone biosynthetic process**	3.39E-03	E
GO:0042425	8,9,7	**choline biosynthetic process**	3.39E-03	E
GO:0017038	5,6,7	**protein import**	3.98E-03	E
GO:0009725	4	**response to hormone stimulus**	5.21E-03	E
GO:0006950	3	**response to stress**	5.66E-03	E
GO:0009853	5	**photorespiration**	5.74E-03	E
GO:0009828	7	**plant-type cell wall loosening**	6.07E-03	E
GO:0009308	5	**cellular amine metabolic process**	6.37E-03	E
GO:0010224	7	**response to UV-B**	6.75E-03	E
GO:0042886	4,5	**amide transport**	6.75E-03	E
GO:0006656	7,8,9	**phosphatidylcholine biosynthetic process**	6.75E-03	E
GO:0015840	5,6	**urea transport**	6.75E-03	E
GO:0042439	7	**ethanolamine and derivative metabolic process**	6.75E-03	E
GO:0042440	3	**pigment metabolic process**	6.77E-03	E

GO:0044271	5	**nitrogen compound biosynthetic process**	7.46E-03	E
GO:0042545	5	**cell wall modification**	9.64E-03	E
GO:0043412	5	**biopolymer modification**	7.47E-03	D
GO:0044260	4	**cellular macromolecule metabolic process**	7.10E-03	D
GO:0034960	5	**cellular biopolymer metabolic process**	4.73E-03	D
GO:0019538	5,4	**protein metabolic process**	3.15E-03	D
GO:0044267	6,5	**cellular protein metabolic process**	2.57E-04	D

Downregulated – MF
No significant results

Downregulated – CC

GO_ID	Level(s)	Term	*P*-value	Enrichment (E)/depletion (D)
GO:0005783	8,7,6,5	**endoplasmic reticulum**	5.14E-06	E
GO:0009527	12,11,10,9,7,8,6,5	**plastid outer membrane**	2.72E-03	E
GO:0009505	6,5	**plant-type cell wall**	4.46E-03	E
GO:0009783	8,6,7,5,4	**photosystem II antenna complex**	4.87E-03	E
GO:0031968	9,8,6,7,5,4	**organelle outer membrane**	8.52E-03	E
GO:0045271	7,6,5	**respiratory chain complex I**	8.80E-03	E
GO:0030964	6,5,4	**NADH dehydrogenase complex**	8.80E-03	E
GO:0019867	5,4	**outer membrane**	9.66E-03	E
GO:0031359	14,13,11,12,10,9,8,7,6	**integral to chloroplast outer membrane**	9.70E-03	E

GO:0031351	10,12,11,9,8,7,6,5	**integral to plastid membrane**	9.70E-03	E
GO:0031355	11,13,12,10,9,8,7,6	**integral to plastid outer membrane**	9.70E-03	E
GO:0012505	4,3	**endomembrane system**	2.75E-03	D

Table S7 Differential expression values (fragments per kilobase of coding sequence per million mapped fragments, FPKM) and relative fold-change in tension wood compared with upright control for all genes involved in the monolignol biosynthesis pathway in *Eucalyptus* (annotation according to V. Carocha *et al.*, in preparation)

PAL	*E. grandis* ID	Average FPKM (upright)	Average FPKM (TW)	Ln (fold change)	*P*-value	*q*-value	Significant
PAL1	Eucgr.A01144	0	0	0.04	0.965	1	No
PAL2	Eucgr.C03570	0	2	3.70	0.0004	1	No
PAL3	Eucgr.G02848	221	154	-0.36	0.4891	0.9336	No
PAL4	Eucgr.G02849	26	27	0.04	0.9077	1.0036	No
PAL5	Eucgr.G02850	54	33	-0.49	0.1354	0.5748	No
PAL6	Eucgr.G02851	10	14	0.26	0.4178	1	No
PAL7	Eucgr.G02852	70	54	-0.26	0.4164	0.9036	No
PAL8	Eucgr.J00907	50	15	-1.23	0.0005	0.0104	Yes
PAL9	Eucgr.J01079	491	253	-0.66	0.7596	0.9987	No

C4H	*E. grandis* ID	Average FPKM (upright)	Average FPKM (TW)	Ln (fold change)	*P*-value	*q*-value	Significant
C4H1	Eucgr.C00065	731	121	-1.80	0.4924	0.936	No
C4H2	Eucgr.J01844	1,397	887	-0.45	0	0	Yes

4CL	*E. grandis* ID	Average FPKM (upright)	Average FPKM (TW)	Ln (fold change)	*P*-value	*q*-value	Significant
4CL1	Eucgr.C02284	948	605	-0.45	0.4957	0.9352	No
4CL2	Eucgr.K00087	42	14	-1.12	0.0008	0.0166	Yes
4CL3	Eucgr.B00135	0	0	-0.21	0.7837	1	No
4CL4	Eucgr.B03468	0	0	-0.19	0.8052	1	No
4CL5	Eucgr.B03502	0	0	0.91	0.2549	1	No
4CL6	Eucgr.B03942	4	6	0.30	0.4114	1	No
4CL7	Eucgr.B03943	9	7	-0.32	0.36	1	No
4CL8	Eucgr.D02624	0	0	0.17	0.8219	1	No
4CL9	Eucgr.F03543	19	18	-0.05	0.8875	1.0049	No
4CL10	Eucgr.G02758	0	0	0.00	0.3085	1	No
4CL11	Eucgr.G02879	0	0	0.00	0.3085	1	No
4CL12	Eucgr.K02927	1	0	-0.31	0.6758	1	No
4CL13	Eucgr.K02929	5	4	-0.27	0.486	1	No

HCT	*E. grandis* ID	Average FPKM (upright)	Average FPKM (TW)	Ln (fold change)	*P*-value	*q*-value	Significant
HCT1	Eucgr.F03972	0	1	0.81	0.2569	1	No
HCT2	Eucgr.F03973	0	0	0.00	0.1679	1	No
HCT3	Eucgr.F03974	0	0	0.00	0.1932	1	No
HCT4	Eucgr.F03978	21	13	-0.52	0.1272	1	No
HCT5	Eucgr.J03126	288	240	-0.18	0.8091	1.0055	No

C3H	*E. grandis* ID	Average FPKM (upright)	Average FPKM (TW)	Ln (fold change)	*P*-value	*q*-value	Significant
C3H1	Eucgr.A02185	15	41	1.01	0.0015	0.0267	Yes
C3H2	Eucgr.A02188	45	77	0.54	0.0902	0.4735	No
C3H3	Eucgr.A02190	741	609	-0.20	0.9166	1.0039	No
C3H4	Eucgr.G03199	316	16	-2.99	0	0.0001	Yes

CCoAOMT	*E. grandis* ID	Average FPKM (upright)	Average FPKM (TW)	Ln (fold change)	*P*-value	*q*-value	Significant
CCoAOMT1	Eucgr.I01134	750	487	-0.43	0.6354	0.9808	No
CCoAOMT2	Eucgr.G01417	1,731	601	-1.06	0.3313	0.8527	No
CCoAOMT3	Eucgr.B02687	0	0	0.00	1	1	No
CCoAOMT4	Eucgr.C00924	0	0	0.00	1	1	No
CCoAOMT5	Eucgr.C00925	0	0	0.00	0.049	1	No
CCoAOMT6	Eucgr.C03667	0	0	0.00	1	1	No
CCoAOMT7	Eucgr.C03668	0	0	0.00	1	1	No
CCoAOMT8	Eucgr.C03674	0	0	0.00	1	1	No
CCoAOMT9	Eucgr.C03680	0	0	0.00	0.1587	1	No
CCoAOMT10	Eucgr.C03684	0	0	-0.43	0.804	1	No
CCoAOMT11	Eucgr.C03939	0	0	0.00	1	1	No
CCoAOMT12	Eucgr.F04260	2	2	0.06	0.8883	1	No
CCoAOMT13	Eucgr.H04643	0	0	0.00	1	1	No
CCoAOMT14	Eucgr.H04644	0	0	0.00	1	1	No
CCoAOMT15	Eucgr.H04646	2	1	-0.76	0.1257	1	No
CCoAOMT16	Eucgr.H04648	3	2	-0.41	0.4372	1	No
CCoAOMT17	Eucgr.H04650	0	0	-0.49	0.6894	1	No

F5H	*E. grandis* ID	Average FPKM (upright)	Average FPKM (TW)	Ln (fold change)	*P*-value	*q*-value	Significant
F5H1	Eucgr.I02371	0	0	0.56	0.588	1	No
F5H2	Eucgr.J02393	1,854	1,362	-0.31	0	0	Yes

COMT	*E. grandis* ID	Average FPKM (upright)	Average FPKM (TW)	Ln (fold change)	*P*-value	*q*-value	Significant
COMT1	Eucgr.A01397	2,908	2,648	-0.09	0	0	Yes
COMT2	Eucgr.A00759	0	0	0.00	0.1587	1	No
COMT3	Eucgr.A01389	0	0	0.00	1	1	No
COMT4	Eucgr.A01392	0	0	0.43	0.7602	1	No
COMT5	Eucgr.A01394	0	0	0.00	1	1	No
COMT6	Eucgr.A01395	0	0	0.00	0.0984	1	No
COMT7	Eucgr.A01600	0	3	1.86	0.0035	1	No
COMT8	Eucgr.A01795	0	0	0.57	0.6618	1	No
COMT9	Eucgr.A01796	0	0	0.11	0.9446	1	No
COMT10	Eucgr.A01797	0	0	-0.70	0.7267	1	No
COMT11	Eucgr.A01846	0	0	-0.93	0.5881	1	No
COMT12	Eucgr.A01863	0	0	0.00	1	1	No
COMT13	Eucgr.A01865	0	0	0.00	1	1	No
COMT14	Eucgr.A01867	0	0	0.00	0.1587	1	No
COMT15	Eucgr.A01873	0	0	0.00	0.1587	1	No
COMT16	Eucgr.A01874	0	0	0.00	1	1	No
COMT17	Eucgr.A01875	0	0	0.00	0.2819	1	No
COMT18	Eucgr.A01876	0	0	-0.20	0.8689	1	No
COMT19	Eucgr.A01877	0	0	0.00	0.2819	1	No
COMT20	Eucgr.A01878	0	0	0.00	0.1587	1	No
COMT21	Eucgr.A01880	0	0	0.00	1	1	No
COMT22	Eucgr.A01881	0	0	2.07	0.1739	1	No
COMT23	Eucgr.A01884	0	0	-0.44	0.6503	1	No
COMT24	Eucgr.A02870	0	1	0.00	0.0317	1	No
COMT25	Eucgr.B01744	1	2	0.36	0.4813	1	No
COMT26	Eucgr.B01747	0	0	-1.19	0.2973	1	No
COMT27	Eucgr.E01092	0	0	0.00	1	1	No
COMT28	Eucgr.E03146	0	0	0.48	0.6355	1	No
COMT29	Eucgr.E03148	0	0	1.29	0.2678	1	No
COMT30	Eucgr.E03339	1	1	0.16	0.8419	1	No
COMT31	Eucgr.E03341	0	1	0.47	0.5956	1	No
COMT32	Eucgr.E03874	1	1	0.50	0.469	1	No
COMT33	Eucgr.E03875	2	3	0.18	0.7015	1	No
COMT34	Eucgr.E03877	0	0	0.00	1	1	No
COMT35	Eucgr.F02623	17	6	-1.06	0.0028	1	No
COMT36	Eucgr.F02624	0	1	1.00	0.1213	1	No
COMT37	Eucgr.F02625	0	0	0.00	0.1587	1	No
COMT38	Eucgr.F03794	8	7	-0.07	0.8654	1	No
COMT39	Eucgr.G00017	0	0	0.00	1	1	No
COMT40	Eucgr.G00020	0	0	0.00	0.1587	1	No
COMT41	Eucgr.G01808	0	0	0.00	1	1	No

COMT42	Eucgr.G01810	0	0	0.00	1	1	No
COMT43	Eucgr.H00347	0	0	0.00	0.2398	1	No
COMT44	Eucgr.H00348	0	0	0.00	1	1	No
COMT45	Eucgr.H00349	0	0	0.00	0.1587	1	No
COMT46	Eucgr.H00350	0	0	0.00	1	1	No
COMT47	Eucgr.H00351	0	0	0.00	1	1	No
COMT48	Eucgr.H00352	0	0	0.00	1	1	No
COMT49	Eucgr.H00353	0	0	0.00	1	1	No
COMT50	Eucgr.H00354	0	0	0.00	1	1	No
COMT51	Eucgr.H00356	0	0	0.00	1	1	No
COMT52	Eucgr.H03920	0	2	1.43	0.0272	1	No
COMT53	Eucgr.H03922	0	0	1.89	0.3266	1	No
COMT54	Eucgr.H03924	0	0	1.40	0.2023	1	No
COMT55	Eucgr.H03926	0	0	-0.23	0.7667	1	No
COMT56	Eucgr.I02810	0	0	0.00	1	1	No
COMT57	Eucgr.K00041	0	0	0.00	1	1	No
COMT58	Eucgr.K00449	0	0	0.00	1	1	No
COMT59	Eucgr.K00949	0	0	0.00	1	1	No
COMT60	Eucgr.K00950	0	0	0.00	0.0786	1	No
COMT61	Eucgr.K00951	419	346	-0.19	0.7944	1.0032	No
COMT62	Eucgr.K00953	0	0	1.02	0.4873	1	No
COMT63	Eucgr.K00954	0	0	0.40	0.7347	1	No
COMT64	Eucgr.K00955	6	0	-3.18	0.0002	1	No
COMT65	Eucgr.K00956	0	0	0.11	0.9199	1	No
COMT66	Eucgr.K00957	1	5	1.29	0.014	1	No
COMT67	Eucgr.K01696	0	0	0.20	0.8643	1	No

CCR	***E. grandis* ID**	**Average FPKM (upright)**	**Average FPKM (TW)**	**Ln (fold change)**	***P*-value**	***q*-value**	**Significant**
CCR1	Eucgr.J03114	518	389	-0.29	0.7706	1.0033	No
CCR2	Eucgr.F03954	0	0	0.00	1	1	No
CCR3	Eucgr.B02222	30	38	0.24	0.4536	1	No
CCR4	Eucgr.C01240	132	36	-1.30	0.0003	0.0062	Yes
CCR5	Eucgr.F03605	0	0	1.22	0.2592	1	No
CCR6	Eucgr.G00052	12	9	-0.23	0.5315	1	No
CCR7	Eucgr.G02325	1	3	1.52	0.0069	1	No
CCR8	Eucgr.I01552	1	0	-0.65	0.4757	1	No
CCR9	Eucgr.I01783	14	5	-0.99	0.0051	1	No

CAD	*E. grandis* ID	Average FPKM (upright)	Average FPKM (TW)	Ln (fold change)	*P*-value	*q*-value	Significant
CAD1	Eucgr.G01350	37	40	0.07	0.8271	1.0018	No
CAD2	Eucgr.H03208	109	68	-0.47	0.1964	0.6745	No
CAD3	Eucgr.D00468	0	0	0.00	1	1	No
CAD4	Eucgr.D00471	0	0	0.00	1	1	No
CAD5	Eucgr.D00472	0	0	0.00	1	1	No
CAD6	Eucgr.D00473	0	0	0.00	1	1	No
CAD7	Eucgr.D01086	0	0	0.00	1	1	No
CAD8	Eucgr.D01087	0	0	0.00	1	1	No
CAD9	Eucgr.D01088	0	0	0.00	0.2398	1	No
CAD10	Eucgr.D01089	0	0	0.00	1	1	No
CAD11	Eucgr.D01090	0	0	0.00	1	1	No
CAD12	Eucgr.D01091	0	0	0.00	1	1	No
CAD13	Eucgr.E01103	0	0	0.28	0.8117	1	No
CAD14	Eucgr.E01104	0	1	1.20	0.101	1	No
CAD15	Eucgr.E01105	2	2	-0.38	0.4649	1	No
CAD16	Eucgr.E01107	9	12	0.28	0.4266	1	No
CAD17	Eucgr.E01108	1	4	1.29	0.0181	1	No
CAD18	Eucgr.E01110	5	16	1.11	0.0002	1	No
CAD19	Eucgr.E01115	0	2	2.16	0.0023	1	No
CAD20	Eucgr.E01117	11	28	0.89	0	1	No
CAD21	Eucgr.E01119	71	75	0.05	0.7962	1.0031	No
CAD22	Eucgr.E02204	0	0	0.00	1	1	No
CAD23	Eucgr.E02310	0	0	0.00	1	1	No
CAD24	Eucgr.E02319	0	0	0.00	1	1	No
CAD25	Eucgr.E02559	0	0	0.00	1	1	No
CAD26	Eucgr.E02570	0	0	0.00	1	1	No
CAD27	Eucgr.E02580	0	0	0.00	1	1	No
CAD28	Eucgr.F01676	0	2	3.35	0.0066	1	No
CAD29	Eucgr.F01677	0	1	1.64	0.1103	1	No
CAD30	Eucgr.F01678	0	1	2.18	0.0675	1	No
CAD31	Eucgr.F01679	0	1	3.47	0.093	1	No
CAD32	Eucgr.F01680	0	1	0.00	0.0478	1	No
CAD33	Eucgr.G02223	0	0	1.17	0.5009	1	No
CAD34	Eucgr.H02411	0	0	0.00	1	1	No
CAD35	Eucgr.H02412	0	0	0.00	1	1	No
CAD36	Eucgr.H02414	0	0	0.00	1	1	No
CAD37	Eucgr.H02415	0	0	0.00	0.1587	1	No
CAD38	Eucgr.H02431	0	0	0.00	1	1	No
CAD39	Eucgr.H02433	0	0	0.00	0.1587	1	No
CAD40	Eucgr.H02434	0	0	0.00	1	1	No
CAD41	Eucgr.H04903	10	20	0.67	0.0094	1	No

CAD42	Eucgr.I00570	5	5	0.06	0.876	1	No
CAD43	Eucgr.I00571	0	0	0.00	0.1587	1	No
CAD44	Eucgr.I00572	0	0	0.00	0.1587	1	No
CAD45	Eucgr.I00573	0	0	0.00	1	1	No
CAD46	Eucgr.K01941	0	0	0.00	0.0786	1	No

Significant differences are highlighted and average expression colouring is scaled within gene families.

Table S8 *Arabidopsis thaliana* homologs significantly differentially expressed between tension wood and the upright control, in this study as well as in *Populus* (Andersson-Gunnerås *et al*., 2006)

Arabidopsis ID	Description	Shared poplar/*Eucalyptus*?	Direction
AT1G05010	EFE (ETHYLENE-FORMING ENZYME); 1-aminocyclopropane-1-carboxylate oxidase	YES	UP
AT1G17950	MYB52 (MYB DOMAIN PROTEIN 52); DNA binding / transcription factor	YES	UP
AT1G54100	ALDH7B4 (Aldehyde Dehydrogenase 7B4); 3-chloroallyl aldehyde dehydrogenase/ oxidoreductase	YES	UP
AT1G62990	KNAT7 (KNOTTED-LIKE HOMEOBOX OF *ARABIDOPSIS THALIANA* 7); DNA binding / transcription activator/ transcription factor	YES	UP
AT2G01940	nucleic acid binding / transcription factor/ zinc ion binding	YES	UP
AT3G27330	zinc finger (C3HC4-type RING finger) family protein	YES	UP
AT3G43190	SUS4; UDP-glycosyltransferase/ sucrose synthase/ transferase, transferring glycosyl groups	YES	UP
AT3G47690	zinc finger (GATA type) family protein	YES	UP
AT5G27030	FLA12	YES	UP
AT1G19300	PARVUS (PARVUS); polygalacturonate 4-alpha-galacturonosyltransferase/ transferase, transferring glycosyl groups / transferase, transferring hexosyl groups	YES	DOWN
AT2G38060	PHT4;2 (PHOSPHATE TRANSPORTER 4;2); carbohydrate transmembrane transporter/ inorganic phosphate transmembrane transporter/ organic anion transmembrane transporter/ sugar:hydrogen symporter	YES	DOWN
AT3G04730	IAA16; transcription factor	YES	DOWN

AT3G06350	MEE32 (MATERNAL EFFECT EMBRYO ARREST 32); 3-dehydroquinate dehydratase/ NADP or NADPH binding / binding / catalytic/ shikimate 5-dehydrogenase	YES	DOWN
AT3G21570	unknown protein	YES	DOWN
AT4G10270	MEE58 (MATERNAL EFFECT EMBRYO ARREST 58); adenosylhomocysteinase/ copper ion binding	YES	DOWN
AT4G13940	F5H (FERULIC ACID 5-HYDROXYLASE 1); ferulate 5-hydroxylase/ monooxygenase	YES	DOWN
AT4G36220	protein binding	YES	DOWN
AT5G07220	remorin family protein	YES	DOWN
AT5G23750	pathogenesis-related thaumatin family protein	YES	DOWN
AT5G37600	ATEB1A; microtubule binding	YES	DOWN
AT5G40020	PIP3 (PLASMA MEMBRANE INTRINSIC PROTEIN 3); water channel	YES	DOWN
AT5G60490	TPR3 (TOPLESS-RELATED 3)	YES	DOWN
AT1G06620	2-oxoglutarate-dependent dioxygenase, putative	NO	
AT2G38080	IRX12 (IRREGULAR XYLEM 12); laccase	NO	
AT3G54810	PLA IIIA (PATATIN-LIKE PROTEIN 6)	NO	
AT3G54950	wound-responsive family protein	NO	
AT4G35100	ATBAG3 (ARABIDOPSIS THALIANA BCL-2-ASSOCIATED ATHANOGENE 3); protein binding	NO	
AT5G14230	ATGSR1; copper ion binding / glutamate-ammonia ligase	NO	

For each ID, the description is provided as well as whether the direction of expression in tension wood relative to the upright control was shared between *Eucalyptus* and *Populus*.

Andersson-Gunnerås S, Hellgren JM, Björklund S, Regan S, Moritz T, Sundberg B. 2003. Asymmetric expression of a poplar ACC oxidase controls ethylene production during gravitational induction of tension wood. *Plant Journal* **34:** 339–349.

Table S9 CAZymes upregulated in tension wood and their relative expression in seven tissues of *Eucalyptus grandis*

Gene ID	Arabidopsis hits	Protein name	CAZyme	Young leaf	Shoot tips	Mature leaf	flowers	roots	phloem	Immature xylem
Eucgr.H00343	AT1G684701		GT47	0%	0%	0%	0%	0%	7%	93%
Eucgr.F00232	AT4G333301	GUX2 , PGSIP3	GT8	1%	3%	2%	3%	5%	11%	75%
Eucgr.C03199	AT3G431901	SUS4	GT4	12%	9%	8%	14%	2%	10%	46%
Eucgr.A00510	AT2G381501		GT32	0%	0%	0%	0%	66%	0%	34%
Eucgr.J01374	AT3G293201		GT35	2%	7%	2%	15%	17%	27%	30%
Eucgr.I01147	AT1G497101	FUCTB, FUT12	GT10	19%	16%	15%	11%	0%	9%	29%
Eucgr.H00536	AT3G178801	HIP, TDX	GT41	12%	11%	9%	14%	4%	25%	25%
Eucgr.K00865	AT4G152401		GT31	11%	24%	14%	13%	0%	15%	24%
Eucgr.F03658	AT1G557401	AtSIP1, SIP1	GH36	23%	13%	10%	9%	2%	23%	20%
Eucgr.E01169	AT4G194201		CE13	16%	5%	30%	10%	1%	19%	20%
Eucgr.B00354	AT1G238701	ATTPS9, TPS9	GT20	18%	20%	12%	9%	13%	9%	18%
Eucgr.B02686	AT1G680201	ATTPS6, TPS6	GT20	16%	24%	13%	15%	14%	8%	10%
Eucgr.F01855	AT1G451301	BGAL5	GH35	19%	13%	27%	19%	1%	11%	9%
Eucgr.I01697	AT3G273301		GT92	23%	19%	22%	21%	1%	7%	6%
Eucgr.B02118	AT5G288401	GME		12%	17%	12%	25%	0%	29%	6%
Eucgr.B00859	AT3G180801	BGLU44	GH1	22%	18%	21%	22%	0%	12%	5%

Data for relative expression is available on EucGeNIE (www.eucgenie.org). Colour intensity indicates relative tissue expression for each gene (white, 0; red, 100%) in each of the seven listed tissues and organs.